National Défense
Defence nationale

LOW-ANGLE TRACKING IN THE PRESENCE OF DUCTING, COHERENT AND INCOHERENT MULTIPATH

by

Éloi Bossé, Ross Turner
and Denis Dion

DEFENCE RESEARCH ESTABLISHMENT OTTAWA
REPORT NO. 1240

Canada

November 1994
Ottawa

National Défense
Defence nationale

LOW-ANGLE TRACKING IN THE PRESENCE OF DUCTING, COHERENT AND INCOHERENT MULTIPATH

by

Éloi Bossé and Ross Turner
Surface Radar Section
Radar and Space Division

and

Denis Dion
Electro-Optic Division
Defence Research Establishment Valcartier

DEFENCE RESEARCH ESTABLISHMENT OTTAWA
REPORT NO. 1240

PCN
041LC

November 1994
Ottawa

LOW-ANGLE TRACKING IN THE PRESENCE OF DUCTING, COHERENT AND INCOHERENT MULTIPATH.

É. Bossé, D. Dion, R.M. Turner

ABSTRACT

This report presents results on recent improvements to the low-angle tracking algorithm based on the Refined Maximum Likelihood (RML) method. Specifically the report describes results obtained for three different models: (1) the RML model; (2) a model which accounts for radar fluctuation of the specular return; (3) a third model which accounts for the effect of ducting. The results indicate that the simple RML model produces better results than obtained by using a model that attempts to account for the incoherent fluctuation in the specular direction. In the case of ducting, under moderate sea state conditions, the parabolic approximation of the Helmholtz wave equation gives accurate tracking while a simple two-ray multipath model (Kerr) is used for standard propagation conditions. For very high sea states, phase monopulse with averaging over a number of estimates at different frequencies gives sufficient accuracy for most applications.

RÉSUMÉ

Nous présentons dans ce rapport les résultats les plus récents sur le pistage de cibles à basse altitude en présence de propagation dite anormale et à trajets multiples. La solution suggérée est d'utiliser le maximum de vraisemblance dont le modèle d'observation prend compte des conditions du milieu: état de mer, conduit d'évaporation, ... etc. Des résultats de simulation et d'expériences dans la bande X sont présentés. Les résultats montrent qu'en présence de conduits d'évaporation pour des états de mer modérés, l'approximation parabolique de l'équation d'onde d'Helmholtz donne un pistage précis alors que dans les conditions normales de propagation un modèle simple à deux rayons suffit. Pour des états de mer très élevés, on recommande d'utiliser la diversité de fréquences avec un monopulse de phase qui donne une précision suffisante pour la plupart des applications.

EXECUTIVE SUMMARY

Recent advances in propagation modeling have led to a higher level of sophistication for radar tracking systems. The problem addressed in this report is that of accurate tracking of low-altitude targets above the sea in the presence of multipath and ducting. The proposed solution is to use multifrequency array-signal processing based on Maximum Likelihood (ML) estimation with an observation model which characterizes the propagation medium and the noise environment.

In previous work we used a model for *specular multipath* in two contexts: Refined Maximum Likelihood (RML) estimation and Eigenvector Analysis using a Multipath Model (EAMM). The results indicated that the RML approach yielded rms tracking errors 4 to 6 times smaller than achieved using Fourier beamforming. As well RML has a lower sensitivity to calibration errors compared with other high resolution algorithms such as the MUltiple SIgnal Classification (MUSIC) .

In this report, two aspects not addressed in previous work are studied: the effect of *incoherent multipath* and the effect of *anomalous propagation* on model fitting techniques such as RML. The approach is to modify the observation model according to the situation. In modelling incoherent multipath, we restrict ourselves to the random variations in the amplitude and phase of the reflected ray coming from the specular direction. Beard [31] has shown that this is the largest contributor to incoherent multipath. The phenomenon of diffuse multipath where the scattered rays arrive from direction far removed from the specular direction is specifically excluded from the model.

Three observation models are compared on the basis of their relative performance in the presence of incoherent multipath: (1) the angle-of-arrival (AOA) model, (2) the refined multipath (RM) model, and (3) the QRM model where a Quadrature term is added to the RM model to account for a random fluctuation in the reflected signal coming from the specular direction. The resulting ML estimation techniques are called MLE, RML and QRML respectively .

In the case of *anomalous propagation*, determination of the signal model requires a rapid computation of the vertical field pattern using the parabolic approximation of the Helmholtz wave equation, here denoted as PEM (parabolic equation method), in

conjunction with a method for estimating prevailing refractivity profiles from readily available standard meteorological parameters. A new model, called WKDMBL (Walmsley-Kel-Defence Research Establishment Valcartier Marine Boundary Layer), is used to estimate the refraction profile; the proposed combination is called WKDMBL-PCPEM.

Two sources of experimental data have been used: (1) the Experimental Low-Angle Tracking (ELAT) 8-element sampled-aperture system; and (2) an X-band experimental Height-Gain Profiler (HGP) with meteorological sensors. Both systems were developed at the Defence Research Establishment Ottawa (DREO). ELAT uses two RF frequencies of 8.6 and 9.6 GHz. ELAT was used to collect data for sea conditions varying from Sea State 0 (SS0) to Sea State 5 (SS5). Unfortunately, we do not have the corresponding meteorological data with the ELAT data. The HGP data, however, includes good quality meteorological data. Therefore the experimental verification of the ducting models was carried out using the HGP data: these data were collected for two beacon frequencies of 8.6 and 9.6 GHz.

For the case of *diffuse or incoherent multipath,* QRML models the physical phenomena more accurately than does RML which assumes specular multipath. Nevertheless, the simulation results indicate that RML produces smaller errors than QRML even when incoherent multipath is present. This is attributed to the following factors: (1) RML exploits the resolution inherent in the interferometer pair made up of the radar and its image in the sea giving an estimation with a much higher resolution than obtainable using QRML; (2) Model errors introduced by using the RML model when the QRML model is more accurate produce biased estimates. These bias errors turn out to be smaller than errors introduced by the much larger variance of the QRML estimator; (4) The RML estimator has been shown to be less sensitive to phase and amplitude calibration errors on the antenna array than QRML.

For almost all the ELAT data analyzed, the following conclusions hold: - Rms tracking errors are reduced by a factor of 4 to 6 by using RML as opposed to Fourier beamforming; - Phase monopulse with frequency averaging performed better than Fourier beamforming with tracking errors only 3 to 4 times as large as those of RML; - RML is very robust to channel mismatches, typically, RML will tolerate gain and phase errors of 25%; - RML works well for both smooth and rough sea conditions.

In the case of *ducting*, the results of simulations indicate that ducting effects must be modeled to attain accurate tracking at ranges greater than 5 km for the typical radar-target geometry encountered in maritime low-angle tracking. However the propagation models are imperfect, there are still some work to be done in the case of rough surfaces. Another difficulty is to find an efficient technique for determining the index of refraction throughout the medium. These difficulties reside in the acquisition of meteorological data and the modelling of the air/sea surface boundary layer.

The results of limited experiments with the HGP indicate that very accurate tracking can be obtained in the presence of multipath and ducting when the propagation conditions are known a priori. However, more extensive experimentation with a real antenna array in conjunction with a meteorological system, where several data vectors at various frequencies can be collected, is required to determine the limitations of the approach in realistic environments. Real-time performance could be obtained by using look-up tables where a large number of scenarios would have been pre-computed.

TABLE OF CONTENTS

LIST OF FIGURES

LOW-ANGLE TRACKING IN THE PRESENCE OF DUCTING, COHERENT AND INCOHERENT MULTIPATH.

1. INTRODUCTION

Recent advances in propagation modeling have led to a higher level of sophistication for radar tracking systems. In recent years a considerable amount of research has been done on array signal processing techniques using superresolution algorithms to separate a target from its image and to provide an accurate estimate of the elevation of the target. We consider an essentially different approach which uses multifrequency Maximum Likelihood (ML) estimation with an observation model that characterizes the propagation medium and the noise environment. The idea is to use as much a priori information in the model as possible for reducing the number of unknown parameters to a minimum and thus increasing the estimation accuracy.

When a radar illuminates a low-altitude target over a flat surface, it receives mainly two signals: one directly from the target and one reflected from the surface. These signals interfere in a constructive or destructive way depending on their relative path length. In previous work [1-3] we used the idea of modeling the interference pattern in the context of the ML estimation theory [1-2] and with an eigenvector approach [3] in two new algorithms: the Refined Maximum Likelihood (RML) technique; and Eigenvector Analysis using a Multipath Model (EAMM).

In [2-3] the performance of the RML algorithm was compared with that obtained with Fourier beamforming and also with the MUltiple SIgnal Classification (MUSIC) [4] technique. The experimental results were obtained over various sea conditions: sea state 0 (SS0) to sea state 4 (SS4). These results indicated that the RML approach gave rms tracking errors 4 to 6 times smaller than achieved using other techniques; as well, RML is less sensitive to calibration errors than the other high resolution algorithms. Note, however, that RML works so well because it exploits frequency agility in an optimal manner. If weighted or unweighted frequency averaging is applied to phase monopulse, acceptable performance can sometimes be obtained for moderate bandwidths [5-6].

In this report, two aspects not addressed in [1-3] are studied: the effects of incoherent multipath and anomalous propagation on model fitting technique such as RML. The approach is to modify the type of observation model according to the situation.

In the case of standard propagation conditions, we analyze the effects of incoherent multipath on low-angle tracking. A rather complete formulation of the problem of ML estimation of target height in specular multipath is given in [2]. The discussion here is restricted to the effect of incoherent multipath on array signal processing techniques. The term incoherent multipath refers to the random fluctuation in amplitude and phase of the signal coming from the specular direction. Beard [7] found that the angular spectrum of incoherent multipath was sharply peaked in the specular direction. Further supporting experimental work is found in Beckmann and Spizzichino [8, pp. 304-305] where signals identified as specular show a strong random fluctuation consistent with the results of Beard [7]. Beckmann and Spizzichino [8] reserves the designation "diffuse" for signals originating well away from the specular direction. There is therefore not an exact correspondence between the incoherent multipath of Beard and what is called diffuse multipath in [8]. In this report, we will compare three observation models used in ML direction finding on the basis of their relative performance in the presence of incoherent multipath:

(1) The angle-of-arrival (AOA) model. Here the model comprises two plane waves having unknown angles of arrival and unknown amplitudes and phases. Signals are superimposed on zero-mean Gaussian receiver noise which is independent from one array element to another but assumed to have the same variance. Where more than one frequency is used the amplitudes and phases are assumed to be independent from one frequency to the next as is typical of a frequency agile radar with sufficient diversity to decorrelate the target cross-section (e.g. Swerling II or IV). With N frequencies, there are $4N + 2$ unknowns. The unknown amplitudes and phases can be eliminated mathematically in the preliminary operations for maximizing the likelihood function; a two-dimensional search over two unknown angles of arrival is necessary to maximize the likelihood function.

(2) The refined multipath (RM) model. The resulting maximum likelihood estimation technique is called RML. Geometric information combined with prior knowledge of the radar height above the sea, target range and sea state allows the derivation of a signal model having a reduced number of unknowns compared with the AOA model: a signal amplitude and phase and the target height. For single frequency operation there are three unknowns

compared with six for the AOA model. With N agile frequencies there are N + 1 unknowns compared with 2N + 2 for the AOA model. The reduced number of unknowns compared with the AOA model results in a lower variance. The better fit to the physical phenomena compared with monopulse results in lower bias errors. The composite signal formed from the superposition of the direct and reflected signals is superimposed on Gaussian receiver noise having the same characteristics as in (1) above. In the RML technique, the unknown amplitudes and phases are eliminated mathematically leaving a one-dimensional search for the target height that maximizes the likelihood function.

(3) The QRM model. A quadrature term is added to the RM model to account for a random fluctuation in the reflected signal coming from the specular direction. The resulting maximum likelihood estimation technique is called QRML. Assumptions concerning the receiver noise and the effects of frequency agility are the same as for (1) and (2) above. A detailed derivation of this model will be given; it will be shown that the likelihood function can be expressed as a function of target height only; therefore only a one-dimensional search is required for the maximum likelihood estimate of target height For single frequency operation, the model has five unknown parameters to estimate; with N agile frequencies, there are 4N + 1 unknowns.

In the case of anomalous propagation, the most frequent "anomalous" condition above the sea is the formation of so-called evaporation ducts which can extend the detection range well beyond the horizon under appropriate conditions. However, as shown in a recent analysis [9], ducting has a significant effect on the interference pattern at all ranges beyond 5 km. Under anomalous conditions the received pattern can greatly differ from the one predicted by using Kerr's formulation and so, significant errors can be produced on the target height estimation using the RML algorithm. To correct the RML tracking errors caused by anomalous propagation, accurate predictions of the received signal patterns must be achieved. This requires a two-stage computation. First, the prevailing atmospheric refraction profile is modeled and then used as input to a propagation model to estimate the relative amplitude and phase received across the array.

The propagation model requires the fine structure of the vertical variation of the refractive index near the surface must be accurately known. A direct measurement is impractical on a routine basis; a high profile resolution is required and rapid fluctuations of the meteorological parameters are hard to filter out. In this situation, one preferably relies on modeling based on the physics of the turbulent transport process near the surface. In

the 60's, Jeske [10] proposed a method to describe the refraction profile in the Marine Boundary Layer (MBL) from only four standard meteorological measurements known as bulk measurements: wind speed, air temperature, air humidity and water temperature. His method has been widely used; the best known implementation is that developed at NOSC by Paulus [11]. More recently, Low and Hudack [12] proposed a new model, called WKDMBL (Walmsley-Kel-Defence Research Establishment Valcartier Marine Boundary Layer), using a method developed by Walmsley [13]. Dion [9] showed that WKDMBL can lead to a significantly better prediction of the interference pattern under a wide range of anomalous conditions. It has therefore been adopted for our application.

Three principal approaches are found in the literature to perform field strength calculations in a marine environment: waveguide mode theory, ray-tracing and the split-step solution of the parabolic approximation of the elliptic Helmholtz wave equation. The waveguide mode method has proved appropriate for signal strength computation at long ranges where only a small number of modes remain persistent. At short and medium ranges, ray-tracing provides better solution [14]. In addition, ray tracing provides the phase function (over the receiving array) that is required by RML. A third technique, the solution of the parabolic wave equation using the split-step Fourier technique, here denoted as PEM (parabolic equation method) [15-16], has received wide acceptance in recent years. It offers high computational performance especially when dealing with medium range, low-level and submillimeter-wave band applications, which correspond to the domain of application of the RML tracking technique. A commercial version, called PCPEM [17], is available for running on a PC with the use of a transputer board. This software has been selected for its convenience.

The proposed solution is then to use a rapid computation of the vertical field pattern using the parabolic approximation of the Helmholtz wave equation method described in [15-16] in conjunction with a method to estimate prevailing refractivity profiles from readily available standard meteorological parameters [9,11]. The proposed combination called WKDMBL-PCPEM, should be efficient for linearly polarized systems and under most evaporation duct conditions which are the most frequent conditions. The technique is also efficient under some subrefractive conditions.

Two sources of experimental data have been used: (1) the Experimental Low-Angle Tracking (ELAT) 8-element sampled-aperture system; and (2) an X-band experimental Height-Gain Profiler (HGP) with meteorological sensors both developed at Defense

Research Establishment Ottawa (DREO). A detailed description of HGP is given in Section 5.2. ELAT uses two RF frequencies of 8.6 and 9.6 GHz and was used to collect data for sea conditions varying from Sea State 0 (SS0) to Sea State 5 (SS5). Unfortunately, we do not have the corresponding meteorological data with the ELAT data. The HGP data, however, includes good quality meteorological data. Therefore the experimental verification of the ducting models was carried out using the HGP data: these data were collected for two beacon frequencies of 8.6 and 9.6 GHz.

The paper is organized as follows: Section 2 presents previous related work; Section 3 describes the RML algorithm and the propagation models; Section 4 gives the results of simulations; Section 5 presents experimental results; and Section 6 presents the conclusions and recommendations. We use the following notation: matrices are represented by bold upper-case letters, vectors by bold lower-case letter, scalars by both upper and lower italic letters. The superscripts, $\hat{}$, *, ^{t}, ^{H}, $|\mathbf{a}|$, denote estimate, conjugation, transposition, conjugation-transposition, and vector norm respectively. Also $C^{M\times N}$ signifies a M×N complex matrix.

2. PREVIOUS RELATED WORK

Barton [18] summarizes the low-angle tracking work up to 1974. His paper reviews a number of methods to combat multipath errors: specifically, the works of White [19], Sherman [20], and some others. Barton reports that for these methods the tracking becomes uncertain at elevation near .25 beamwidth. More recently Haykin and Kesler [21-22] propose an adaptive canceler and Haykin [23] investigates the use of high resolution techniques such as autoregressive, maximum entropy and linear prediction. Most high resolution techniques require an angular separation of at least 1/4 of an antenna beamwidth.

The idea of modeling the interference pattern for low-angle tracking is not new. Sherman (1971) [20] used the a priori knowledge of the complex reflection coefficient with a technique named "complex indicated angle". The "complex indicated angle" technique was defined in the context of monopulse. Rook and Litva (1982) [24] used the idea of a detailed propagation model. They designed an algorithm called the CHA (Correlation Height Analysis) for processing the outputs of an array. The CHA finds the maximum correlation between the simulated radar signatures for different target heights and the received signal. The resulting correlation function is ambiguous in height. The true target height is found by using a perturbation technique on the transmitted frequency or on the

receiving antenna height. However, neither the "complex indicated angle" technique nor the CHA technique is based on an optimization criterion.

In the RML approach [1-2], a detailed propagation model is used and the information is treated in an optimal way using the ML criterion. Turner and Bossé [1-2, 25] have analyzed in detail the problem of ambiguities introduced by the large number of ambiguous grating lobes characteristic of the interferometer such as the radar and its image. Frequency agility has been included in the ML optimality criterion itself and shown to be an intrinsic requirement for proper functioning of the RML. Specifically, the height ambiguity problem can be solved by using an array radar with sufficient bandwidth and at least two different frequencies [25].

A discussion of various ML solutions to the problem of low-angle direction finding is provided in [26]. The conclusion of the investigation is that the solutions by Haykin and Reilly [27-28], Howard [29], and White [19] are equivalent. They are special cases of the solution by Ksienski and McGhee [30]. The difference between all these techniques and ours is that they model multipath with two signals: one coming from the target and the other coming from its image, each having an independent phase and amplitude. We use a priori knowledge of target range, frequency, radar height above the sea, sea state, and propagation conditions to refine the multipath model. This reduces the dimensionality of the estimation problem and has a beneficial effect on precision; in general, lack of knowledge of multiple parameters leads to degradation in the performance of any estimator [31, p.84]. Another important benefit is the reduction to a one-dimensional search for the unknown target height; this significantly reduces the computational load in comparison with standard implementations of ML estimation.

3. THE RML ALGORITHM

The RML algorithm has been described extensively in [1-3]. Here, we present only the general observation model and the final form of the algorithm. The signal variation over a vertical array is written as

$$\mathbf{s}_m = b_m \mathbf{f}_m(h) + \eta_m \tag{1}$$

Here $\mathbf{f}_m$ is the model vector, h is the target height, b_m is an unknown complex constant and η_m is the vector of complex receiver noise over the array. The subscript m

indicates the frequency in the case of frequency agility and the vectors $(\mathbf{s}_m, \mathbf{f}_m, \eta_m) \in C^{K\times 1}$, $b_m \in C^{1\times 1}$ and where b_m can be deterministic (non-fluctuating case) or random (fluctuating case). The noise vector η_m is assumed to be stationary, additive, spatially white and independent of the target signals. The quantity K represents the number of sensors. The vector $\mathbf{s}_m$ is called a snapshot of the antenna array outputs.

The ML estimator of the target height is the value of h that maximizes the following function:

$$\mathrm{RML}(h) = \frac{1}{\sum_{m=1}^{M} \frac{|\mathbf{s}_m|^2}{\sigma_m^2}} \sum_{m=1}^{M} \frac{|\mathbf{s}_m^H \mathbf{f}_m(h)|^2}{\sigma_m^2 |\mathbf{f}_m(h)|^2} \qquad (2)$$

By using the Cauchy-Schwartz inequality, we can show that $0 \le \mathrm{RML}(h) \le 1$.

This form of the RML estimator, (2), is appropriate for a frequency agile radar with m=1 to M different frequencies. This estimator implicitly assumes that coherent integration occurs for each of the M frequency bursts prior to the estimation process. Equation (2) can also be used for processing non coherent vectors where the summations are extended over all the data vectors. The RML estimator as given by (2) applies to the non-fluctuating case and may be applied to the fluctuating case if we consider b_m as being constant for N snapshots taken at a given frequency [2, p. 817].

In (2), $\mathbf{s}_m$ is the coherently integrated data vector and σ_m^2 is the receiver noise power corresponding to the m^{th} frequency for a frequency agile radar. The vector product inside the summation sign in the numerator of (2) is analogous to a Fourier transform of the array outputs; indeed when the reflection from the sea becomes vanishingly small in the case of very rough seas, this inner product does reduce to the Fourier transform. A search must be carried out over the expected values of h to determine the maximum of RML(h) which is the RML estimate of the target height. This means that the position of the target must be roughly determined using standard techniques followed by a fine search over h to determine the RML estimate.

3.1 Observation Models

Maximum Likelihood Estimation (MLE) is used to accurately estimate the target height in the presence of multipath under various propagation conditions. MLE is a model fitting technique where the model parameters are chosen to maximize the likelihood function. This section presents various types of observation models and their dependence on the operating environment.

3.1.1 Standard Propagation and Specular Multipath

The method described by Kerr [32] to represent the interaction between direct and reflected signals is used to compute the $\mathbf{f}_m$ functions in (1). It requires knowledge of target range and reflection coefficient . The target range can be initially obtained from an acquisition radar and then maintained as part of the track update process. The reflection coefficient (amplitude and phase) must be computed taking into account the specular scattering coefficient which is a function of sea state. In Kerr's method, standard atmospheric refraction is assumed and modeled by using an effective earth radius (4/3 greater than the actual earth radius); this is usually done in radar analysis to simplify computation or when no a priori information on the refractive structure of the atmosphere is available.

Hence, using Kerr's representation, the noise-free observation model for a signal received at the k^{th} element of an array of K sensors can be written as:

$$v_k = b\, f_k(h) \tag{3}$$

with

$$f_k(h) = e^{-j\frac{\xi}{2R}(z_k^2 + h_k^2)}\left[e^{j\frac{\xi}{R}(z_k h_k)} + A_2\, e^{-j\frac{\xi}{R}(z_k h_k)}\right] \tag{4}$$

and where $\xi = 2\pi/\lambda$. Here λ is the wavelength, z_k is the height of the k^{th} element, R is the target range, and b is an unknown complex amplitude described by (3b) of [2]. The parameter h_k is the target height as viewed from the k^{th} array element and includes a correction for the spherical earth; this varies with the array element height - hence the index k. The complex amplitudes of the direct and reflected rays are simply related by a complex

multipath reflection coefficient A_2. Coefficient A_2 is determined from the reflection and specular scattering coefficients and divergence factor. Computing $f_k(h)$, for k=1,K sensors, using (4) gives the deterministic multipath model vector $\mathbf{f}(h)$ used in (2) where h is the target height with respect to sea surface.

3.1.2 Standard Propagation and Specular + Incoherent Multipath

Diffuse and incoherent multipath appears when the smooth reflecting plane becomes rough. From the viewpoint of geometrical optics, each segment of the path will have facets which meet the condition of equal angles of incidence and reflection between the target and the radar. Hence, the reflected signal will be composed of a combination of reflections from all portions of the surface beneath the direct path. While the specular component has a well-defined amplitude, phase and angle-of-arrival relationship with the direct ray, the diffuse component arising out of the random fluctuations in the reflecting surface is best modeled statistically.

Diffuse multipath can be modeled by using the glistening surface approach developed by Beckmann and Spizzichino [8]. The glistening surface is that part of the earth's surface which can participate in the reflection of the waves for a given position of the transmitter and receiver. Fig.1 shows a typical example of a glistening surface where the shaded area represents the surface producing the diffuse scattering. The total diffuse multipath power received has been derived in [8, p.261] when the radar and the target are at the same altitude ($h1$=$h2$). The diffuse power is then given by

$$P_{diffuse} = |\rho_0|^2 \int_{\xi_a}^{\pi-\xi_a} f(\xi)\, d\xi \tag{5a}$$

with

$$\frac{\sin^2 \xi_a}{\cos \xi_a} = K_\beta \tag{5b}$$

and

$$f(\xi) = \frac{2}{\pi} K_\beta \frac{1}{\sin^3 \xi} \sqrt{1 - \left(K_\beta \frac{\cos \xi}{\sin^2 \xi} \right)^2} \tag{5c}$$

where $f(\xi)$ represents the distribution of the energy scattered by the points of the earth's surface along the transmitter-receiver link.

The parameter K_β plays a dominant role in the study of diffuse scattering. The parameter K_β is the ratio of the grazing angle of a ray that is specularly reflected to the maximum slope βo of the irregularities of the surface. For the frequent case where $K_\beta << 1$, the expression $1-K_\beta/2$ represents the section of the radio path intercepted by the glistening surface. In Fig.2 we have plotted the function $f(\xi)$ for different values of K_β. Depending on that value of K_β, diffuse scattering may occur in the following forms:

1) if $K_\beta << 1$, corresponding to a rough surface, the scattered energy comes primarily from two regions: one near the target and one near the radar.

2) if $K_\beta = 1$, corresponding to a moderately rough surface, the scattered energy is uniformly distributed in a zone surrounding the point of reflection.

3) and when $K_\beta >> 1$, corresponding to a smooth surface, we approach the case of specular multipath with a single reflection point located at $\xi = 90$ degrees.

If the link is asymmetrical ($h1 \neq h2$), this description is only approximate. According to [8, p.264], the mean absolute square of the diffuse scattering is obtained by integrating the function $f(\xi)$ in Fig.2 from 0 to π. The value of the integral in (5a) is

$$\begin{aligned} &\approx 1 \quad for \quad K_\beta > 1 \\ &\approx \frac{1}{2} \quad for \quad K_\beta << 1 \end{aligned} \tag{5d}$$

This value must be multiplied by the Fresnel reflection power $|\rho_o|^2$ to give the total diffuse power. This is valid for an asymmetrical link as well [8, p.265].

In the case of a rough surface ($K_\beta << 1$), Fig.2 shows that the greatest energy densities occur near the two ends of the path. Considering the curvature of the earth for the distant component and the reduced antenna gain for the components just below the radar, the model may in general be represented by Fig.3 (courtesy of [33], p.132). The direct signal is reflected by the target at point T with altitude h, the specular component is formed by its image at point T' with altitude -h, and the reflections coming from the glistening surface contribute to the formation of the diffuse image of the target as shown by the shaded curve.

The distribution of energy as shown in Fig.2 is symmetrical about the specular reflection point. Viewing the illuminated surface as an antenna as in Fig.3 gives a phase center at the specular point. Provided one is in the far-field of this "antenna", the radiation

emanating from it should appear to come from its phase center. Of course for very rough surfaces and high grazing angles the illuminated surface extends very far towards the radar so that this far-field condition is not satisfied. Moreover the surface of this "antenna" is randomly perturbed and constantly changing. Thus one would expect the phase center to move around in a random fashion with its average near the specular point. However, for the conditions of interest involving tracking of targets at very low angles of incidence, the incoherent component of this illumination comes from the region of the specular point primarily within the first Fresnel zone as observed by Beard [7] for values of $\sigma_h \sin(\psi)/\lambda$ up to 78 milliradians. By comparison, the value of $\sigma_h \sin(\psi)/\lambda \approx 80$ milliradians is calculated for the Sylt experimental data taken over the 9.63 km path under sea state 5 conditions. The effective aperture width used in calculating the far field of the illuminated surface when viewed as an antenna is reduced by the sine of the grazing angle ψ, which is quite small for the cases of interest.

THE QRML ALGORITHM

The QRML algorithm is developed to account for an incoherent component coming from the specular direction superimposed on a steady non fluctuating specular component. This is equivalent to assuming that the complex reflection coefficient is unknown and must be estimated. In developing the maximum likelihood estimator for this signal model, we make use of the same a priori information used in the RML algorithm.

The observation model is given by

$$\mathbf{s}_m = a_{1m}\mathbf{f}_m(h) + a_{2m}\mathbf{u}_m(\phi(h)) + \mathbf{n}_m \tag{6}$$

where

$$\mathbf{u}_m(\phi(h)) = \left[1, e^{j\zeta_m du}, \ldots, e^{j\zeta_m N du}\right] \tag{6a}$$

and where $u = \sin(\phi(h))$, $\phi(h)$ is the angle to the reflection point, $N=K-1$, $\zeta_m = 2\pi/\lambda_m$, and d is the spacing between elements. When the target range and radar height are known, $\phi(h)$ can be calculated as a function of the target height, h.

Specular multipath is modeled as $\mathbf{f}_m(h)$, the same as for RML. The incoherent component is modeled as $a_{2m}\mathbf{u}_m(\phi(h))$, a single ray emanating from the specular reflection point with an unknown amplitude and phase, a_{2m}. The noise vector $\mathbf{n}_m$ is white and has equal power in each channel.

The ML estimate of the unknown parameter vector, given the observation set $\{\mathbf{s}_m; m=1, \ldots, M\}$ for M frequencies, is obtained by minimizing the following function:

$$L(h) = \sum_{m=1}^{M} |\mathbf{s}_m|^2 \left(1 - \frac{\mathbf{s}_m^H \mathbf{F}_m (\mathbf{F}_m^H \mathbf{F}_m)^{-1} \mathbf{F}_m^H \mathbf{s}_m}{|\mathbf{s}_m|^2}\right) \tag{7}$$

We apply QR decomposition to obtain

$$\mathbf{F}_m = \mathbf{Q}_m \mathbf{R}_m \tag{7a}$$

$\mathbf{R}_m$ is a 2×2 upper-triangular, non-singular matrix. $\mathbf{Q}_m$ is constructed using Gram-Schmidt orthogonalization, as

$$\mathbf{Q}_m = [\mathbf{q}_{1m}, \mathbf{q}_{2m}] \tag{7b}$$

$$\mathbf{p}_{1m} = \mathbf{f}_m(h) \tag{7c}$$

$$\mathbf{q}_{1m} = \frac{\mathbf{p}_{1m}}{|\mathbf{p}_{1m}|} \tag{7d}$$

$$\mathbf{p}_{2m} = \mathbf{u}_m(\phi(h)) - \frac{\left[\mathbf{f}_m^H(h)\mathbf{u}_m^H(\phi(h))\right]\mathbf{f}_m(h)}{|\mathbf{f}_m(h)|^2} \tag{7e}$$

$$\mathbf{q}_{2m} = \frac{\mathbf{p}_{2m}}{|\mathbf{p}_{2m}|} \tag{7f}$$

After some manipulation, (7) becomes

$$\mathrm{QRML}(h) = \mathrm{RML}(h) + \frac{1}{\sum_{m=1}^{M} |\mathbf{s}_m|^2} \sum_{m=1}^{M} \left|\mathbf{q}_{2m}^H(h)\mathbf{s}_{(m)}\right|^2 \tag{8}$$

The ML estimate is the value of h that maximizes (8). Fig.4 shows QRML(h) calculated for a target range of 5 km, a target height of 40 m, a vertical array of 8 sensors equally spaced between 15 and 16 m above the sea, two transmitted radar frequencies of 9 and 10 GHz and a smooth sea. The multiple peaks represent the RML portion of (8); the

solid line represents QRML. The second term on the right side of (8) destroys the high-resolution, interferometer property of the RML algorithm.

Classical Maximum Likelihood Estimation (MLE)

The following paragraph develops the MLE procedure for the general AOA model with an unknown angle of arrival and complex amplitude for each signal in the model. Multipath is represented by two signals: a direct signal with complex amplitude, a_{1m}, and angle-of-arrival, φ_1, and a reflected signal with a_{2m} and φ_2. In maximizing the likelihood function, the unknown complex amplitudes are eliminated mathematically. This leaves a two-dimensional search for the unknown AOAs that maximize the likelihood function. The observation model is given by

$$\mathbf{s}_m = a_{1m}\mathbf{f}_{1m}(\varphi_1) + a_{2m}\mathbf{f}_{2m}(\varphi_2) + \mathbf{n}_m \tag{9}$$

where $\mathbf{f}_{1m}$ and $\mathbf{f}_{2m}$ are the direction vectors and can be easily obtained by replacing $\phi(h)$ in (6a) by φ_1 and φ_2 respectively. The function to be minimized is given by (7) but now with $\mathbf{F}_m = [\mathbf{f}_{1m}(\varphi_1), \mathbf{f}_{2m}(\varphi_2)]$. The ML estimates are the values of φ_1 and φ_2 that maximize the second term in (7):

$$\mathrm{MLE}(\varphi_1,\varphi_2) = \sum_{m=1}^{M} \frac{K\left|\mathbf{f}_{1m}^{H}\mathbf{s}_m\right|^2 - 2\mathrm{RE}\left(\mathbf{s}_m^{H}\mathbf{f}_{1m}\mathbf{f}_{1m}^{H}\mathbf{f}_{2m}\mathbf{f}_{2m}^{H}\mathbf{s}_m\right) + K\left|\mathbf{f}_{2m}^{H}\mathbf{s}_m\right|^2}{|\mathbf{s}_m|^2\left(K^2 - \left|\mathbf{f}_{1m}^{H}\mathbf{f}_{2m}\right|^2\right)} \tag{10}$$

This is the multiple-snapshot version, frequency-agile, of the estimator described by Howard [29]. MLE provides a resolution comparable to that of QRML as will be shown.

3.1.3 Anomalous Propagation and the parabolic equation (PE) approach

The most frequent "anomalous" condition above the sea is the formation of so-called evaporation ducts which are mostly known to extend the detection range well beyond the horizon under some conditions. However, as shown in a recent analysis [9], apart from the significant effect on signal level at long ranges, ducts significantly affect the interference pattern - as caused by the addition of direct and reflected signals - even at short ranges in the line-of-sight region.

In Fig.5, which shows low-level vertical interference patterns for X-band, we observe that the null positions shift downward as the duct height increases (only the lowest null is shown in the figure). The duct height is a simple means commonly used to characterize ducting conditions. Under subrefractive conditions, which are much less frequent, we note that the nulls shift upward. Fig.6 shows the effects of ducting on the propagation factor versus range. Cases of duct heights of 0, 5, 10 and 15 m are shown. The target height and the receiver height are 25 and 20 m, respectively. We observe that nulls move outward in range as a function of duct height and that the null displacement becomes significant at ranges as close as 5 km. Since in current versions of the RML algorithm the signal received over a vertical array is correlated with patterns that are modeled assuming standard propagation, one can expect target height estimation errors which increases with range.

We have seen that under anomalous conditions the received pattern can greatly differ from the one predicted by using Kerr's formulation and so, significant errors can be produced on the target height estimation. Fig.5 shows the effect of ducting and subrefraction on the vertical interference pattern. To correct the RML tracking errors caused by anomalous propagation, accurate predictions of the received signal **f** patterns must be achieved. This requires a two-stage computation. First, the prevailing atmospheric refraction profile shall be modeled and then used as input to a propagation model to estimate the relative amplitude and phase received over the array.

WKDMBL computes a temperature, wind speed and water vapor profile using a logarithmic equation which incorporates an air stability dependence correction. This correction, whose gradient formulation is called the stability function, characterizes the profiles. For unstable conditions (when the air is cooler than the water, the most frequently occurring conditions), the Businger-Dyer function [34] (called Rossby-Montgomery profile by Jeske [10]) is used for the temperature and the water vapor while a modified KEYPS function as suggested by Businger et al. [34] is used for the wind. For stable conditions (air warmer than water), a Monin-Obukhov log-linear function is used for the three atmospheric parameters. The profile's parameters, such as the stability length, the roughness length, etc., are evaluated following the Walmsley's iterative method [13]. Finally, WKDMBL computes the desired refractivity profile from the temperature and water vapor profiles using a polynomial approximation to describe the atmospheric pressure variation.

The elliptic Helmholtz equation, which describes the propagation of linearly polarized radiation over the earth's surface, is derived from Maxwell's equations. The scalar wave equation for a field component, $\Psi(R,h)$, dependent on range R and height h, is given by:

$$\frac{\partial^2 \Psi}{\partial h^2} + \frac{\partial^2 \Psi}{\partial R^2} + \kappa^2 n^2 \Psi = 0 \tag{11}$$

where κ is the free space wave number and $n(R,h)$, the refractive index.

Analytical solutions of (11) are only possible if κ is independent of R. Furthermore, a direct numerical solution is intractable because (11) is an elliptic partial differential equation which must be numerically solved over the entire propagation domain simultaneously. A tractable solution is a reduction from elliptic to parabolic equation. The parabolic equation approach applies a full-wave, forward-scatter model capable of predicting the propagation for arbitrary atmospheric refractivities. The derivation of the split-step Fourier method for efficient numerical solutions has been presented in [15-16].

To express the field Ψ in terms of an attenuation function f, the reduction from elliptic to parabolic equation is written:

$$\frac{\partial^2 f}{\partial h^2} + 2j\kappa \frac{\partial f}{\partial R} + \kappa^2 (m^2(R,h) - 1) f = 0 \tag{12}$$

where:

$$\Psi(R,h) \approx f(R,h) \frac{e^{j\kappa R}}{\sqrt{R}} \tag{13}$$

where f is a complex number having amplitude and phase which is used in our application. The parameters R and h denote range and elevation, respectively, m is the modified index of refraction which accounts for the earth's curvature and κ is the free space wave number.

The main assumptions required in this reduction from an elliptic to a parabolic form are that the refractive index variations are small on the scale of a wavelength and that the fractional change in $\partial f/\partial R$ over a wavelength is small. These conditions are nearly always satisfied in the troposphere for low elevation angles. The importance of the reduction to a parabolic form is that a numerical solution is easier to compute, in particular by using the

"split-step" algorithm described in [15-16] which exploits the fast Fourier transform technique. This approach has been applied to the sonar problem and recently to RF and millimeter-wave tropospheric propagation. It is applied here to compute **f** in (1) to eliminate bias errors caused by ducting when the two-ray method of Kerr is used to compute **f**.

Domain of validity

The validity of the proposed solution depends on the validity of both the selected MBL models and the PEM code used. WKDMBL is known to be efficient for describing most evaporation duct conditions and subrefraction conditions when the air stability is not too high (i.e. when the ratio of the air-sea temperature difference and the wind speed is low). WKDMBL, and any other models to our knowledge, cannot reliably deal with highly stable conditions (low wind speed and high air-sea temperature difference) and conditions where influential surface-based ducts prevails. However, it is worth mentioning that these conditions, under which WKDMBL's validity degrades, are infrequent in an open sea environment; they mostly occur in coastal and in-land sea.

The PEM approach has difficulty incorporating the effect of the surface on the reflected radiation component, particularly when wave height is significant. The use of PEM should restricted to low sea state conditions when horizontal polarization is used, as in this case, causing the reflection coefficient to be very close to 1 over the whole RF spectrum. Also, some PEM implementations are not valid when multiple reflections occur as in the case of surface-based duct conditions; the PCPEM implementation is not valid for surface-based duct conditions.

However, sea state mainly affects the amplitude of the reflected signal while in RML the absolute amplitude value is not necessary; instead, we require accurate relative amplitude and phase values across the antenna aperture. Thus, in the presence of a rough surface, the global shape of the interference pattern, in particular the position of nulls, is not expected to be significantly affected, and therefore should not affect RML prediction. Therefore, moderate sea states should not cause major errors. For very high sea states (SS5 and up), though, where most of the reflected signal is from diffuse reflections, the use of phase monopulse averaged over the agile frequency band [6] is recommended instead of RML.

Consequently, the proposed WKDMBL-PCPEM combination should be accurate mainly for horizontally polarized systems, for the most commonly occurring evaporation duct conditions and for some subrefraction conditions. For vertical polarization, PCPEM restricts the use of the same reflection coefficient value for computing the contribution of all the bounds inside the evaporation duct. This is accurate enough for horizontally polarized systems since the reflection coefficient is very close to 1 for large deviations of the grazing angle but this introduces errors with the vertical polarization since the reflection coefficient rapidly varies with respect to the grazing angle. It is expected that in the near future models will be improved and made capable of dealing with the other types of atmospheric conditions of interest, notably the strong stable conditions and the conditions dominated by the presence of surface-based ducts. A system design should then be made flexible so that propagation and atmospheric models (PEM and MBL) can be readily upgraded as model enhancements or extensions become available.

A drawback of the proposed WKDMBL-PCPEM solution is the extensive computation demanded for RML where pattern computation is required for each antenna element. For an operational system, one could envision deriving simple approximate formulas to compute the vertical patterns (amplitude and phase), as proposed by Imbeau et al. [35]. In this report, however, we consider only the potential to minimize target tracking errors.

4. RESULTS OF SIMULATION

The simulation results will be presented in two parts. First, we have carried out a comparative performance evaluation of the RML, QRML and MLE methods by means of a Monte-Carlo simulation. The simulation is carried out with a target at a range of five km and at an altitude of 40 m above the sea. The objective is to investigate the effect of diffuse and incoherent multipath on performance. In the second part, we investigate the effects of the evaporation ducting on low-angle tracking and more specifically on model-based algorithms such as RML.

4.1 The effect of diffuse and incoherent multipath on the tracking performance

The simulation of the effects of diffuse multipath relies heavily on the experimental results of Beard as discussed in the introduction. Beard found that approximately 60 % of the incoherent multipath power came from the first Fresnel zone. A similar distribution of

diffuse power is implemented in the simulation. For a given sea state and radar target geometry, the parameter $\sin(\psi)/\lambda$ is calculated and then used to determine ρ_d using Beard's curves [7]. We then determine $\rho_{d1}^2 = fr1 \times \rho_d^2$ and $\rho_{d2}^2 = fr2 \times \rho_d^2$ where $fr1$ and $fr2$ are two adjustable parameters; for instance, Beard uses $fr1 = 0.6$ and $fr2 = 0.4$ in his experiments. Gaussian random numbers, N_1 and N_2 are generated with variances of ρ_{d1}^2 and ρ_{d2}^2. N_1 is added to ρ_S to create a random variation in signal energy consistent with, for instance, 60 % of the incoherent multipath energy coming from the specular direction. This gives a Ricean distribution for ρ_s. Two independent values of N_2 are used to generate the Rayleigh amplitude of a diffuse component having a direction of arrival which is given a uniform probability of lying in the region between the radar horizon and the radar but excluding the first Fresnel zone. The phase of this diffuse component is selected according to the difference between its path length and the direct path between the target and radar.

The results are presented in Figs.7-9 where we determine the root-mean-square-error (RMSE) for target height estimation from 100 Monte Carlo trials. The term SNR, in Figs.7-9, is a per-element signal-to-noise ratio. This term is calculated for a single snapshot at each frequency and is summed over the number of frequencies:

$$\mathrm{SNR_{dB}} = 10 \log \left\{ \sum_{m=1}^{M} \frac{|b_m \mathbf{f}_m(h_t)|^2}{2K\sigma_m^2} \right\} \qquad (14)$$

where M is the number of frequencies, h_t = target height, σ_m^2 is the noise power and $\mathrm{b_m}$ is the complex signal amplitude at each element.

Fig.7 presents three curves labeled: RML, QRML, and MLE. Each of the three algorithms used two snapshots, one for each radar frequency, to estimate the target height. Fig.7 shows the results obtained for a relatively smooth sea (SS2) when no incoherent component was simulated. It is evident that RML performs much better than did QRML or MLE. We conclude that when the incoherent component is not present the use of a priori knowledge of the reflection coefficient significantly increases the tracking accuracy. The performance depends on the separation between the target and its image. For a target separated by half of a beamwidth from its image and an SNR of 10 dB, RML gave RMSE (Root Mean Square Error) on target-height estimates approximately 10 times more accurate than obtained using classical MLE or QRML.

Fig.8 shows the results when 60% of the incoherent power comes from the first Fresnel zone and 40% outside of the first Fresnel zone under SS3-SS4 conditions. In this case both MLE and QRML show larger bias errors and larger variance than RML. The bias errors may be explained by inaccuracy in the observation model which assumes that there are two signals present when in fact there are three signals in the simulation: the direct signal, one from the first Fresnel zone and another one coming from out of the first Fresnel zone. Fig.9 shows the results when 90% of the incoherent power is coming from the first Fresnel zone. Here the bias errors are reduced significantly since the observation model of two signals better represents the observed data when only 10% of the incoherent power is coming out of the first Fresnel zone. The use of an observation model comprising three signals is impractical for the real-time naval low-altitude tracking problem.

Fig.10 illustrates the sensitivity of the different algorithms to array calibration errors. These results show important differences between algorithms; RML is much less sensitive to calibration errors than either MLE or QRML. This sensitivity to calibration errors is a likely explanation for the poor performance of QRML with experimental data.

Figs.10a and 10b show the effect of In-phase (I) and Quadrature (Q) gain and phase imbalances on the tracking performance. Fig.10a presents the results when a gain imbalance, given in percentage, is present. Fig. 10b gives the corresponding figure for the phase imbalance. A Gaussian random generator was used to simulate the errors. The last two parts of Fig.10, (c) and (d) show the effect of misalignment of the eight receiving channels of the vertical array. Here, each channel has its own I and Q receivers which are perfectly orthogonal. These results clearly demonstrate that the RML algorithm is much more robust to calibration errors or to channel mismatches than the classical MLE or QRML (MLE and QRML perform nearly the same - results for QRML only are given in Fig.10). RML can tolerate up to a 25% gain error and up to 24 degrees of phase error while MLE and QRML have a much lower tolerance to channel mismatches. This is obviously important for practical systems; very precise calibration is always difficult to achieve.

4.2 The effect of ducting on the tracking performance

In this section, we evaluate through simulation the tracking error caused by the presence of evaporation ducts when using the current RML technique (i.e. with the assumption of standard propagation). The functional diagram of the simulation is presented in Fig.11. For a specified array antenna, the parabolic equation method (PEM)

is used to simulate received signals, vector **s** in (2), under various ducting conditions, considering an inbound target flying at a constant altitude.

For the conditions under study, the refraction profiles are modeled using the neutral case profile formulation:

$$M(h) = M_0 + 0.125\, h - 0.125\, \delta \ln \frac{h + h_0}{h_0} \qquad (15)$$

where M is called modified refractivity (= $(n\text{-}1) \times 10^6 + .157\, h$, where n is the index of refraction), δ is the duct height and h the elevation, both expressed in meter. M_0 is the surface refractivity arbitrary made equal to 350 and h_0, the aerodynamic roughness parameter, is constant at 1.5×10^{-4} m.

Noise-free signals were considered in order to isolate the effects of ducting. The effect of noise on the RML algorithm has already been investigated using extensive Monte-Carlo simulations [1-3]. Within RML, the model vector $\mathbf{f}(h)$ is calculated using (4), assuming no ducting, over a window of discrete potential heights from h=1,..., H_{max}.

Fig.12 shows the RML target height estimation for a 10-m duct and a target flying at 25 m above the water surface. The antenna array, located at 10 m above the surface, is composed of 16 sensor elements distributed over a 2-m aperture and the two RF frequencies used are 9 and 10 GHz. The bottom graph presents propagation factors for the lowest antenna element. The solid line is the propagation factor value for the simulated condition (duct height = 10 m) while the dotted line is the model vector $\mathbf{f}(h_t)$ value (i.e. corresponding to standard propagation condition). We observe that the respective crest and trough positions start diverging significantly from about 4 km and that from this range increasing tracking errors are obtained, as shown in the upper graph. Although not shown here, one expects that the magnitude of the error will be dependent upon the antenna-target geometry and radar parameters.

Fig.13 shows tracking errors for duct heights of 0, 5, 10, 15 and 20 m using the same radar-target geometry and specifications. The general trend of tracking errors is to increase progressively with target range and duct height. However, at some particular ranges, the target height estimates fall far from the general trend. We observe that this happens at ranges where the signal and calculated nulls positions are so displaced that ambiguities

occur in the search process for the target height. The problem of ambiguities in height estimation is thoroughly discussed in [25].

5. EXPERIMENTAL RESULTS

The experimental results will be presented in two parts. First, we present examples of experimental target tracking using the ELAT system over smooth and rough sea conditions but with no a priori knowledge of the propagation conditions. The second part presents examples of tracking with experimental data in the presence of multipath and ducting using the Height Gain Profiler (HGP) and a measure of the refractivity profile.

5.1 Tracking over rough seas with RML or QRML

Examples of experimental target tracking using the ELAT radar system are presented. ELAT (see details in [1-3]) was developed at DREO as part of a research program to evaluate array signal-processing techniques for tracking aircrafts and missiles flying low over the sea.

The various representative examples presented in this section provides results on:

- the robustness of RML with respect to rough sea conditions,
- the comparative performance of RML and QRML,
- the robustness of RML and QRML with respect to calibration errors,

In this section we compare the tracking performance of RML and QRML in the presence of diffuse multipath. The simulation results from section 4 showed that QRML is much more sensitive to calibration errors than RML. Calibration errors in the ELAT system may have caused the poor performance of QRML.

Most of the rough sea data used in the evaluation was obtained from an experiment carried out during autumn, 1990, on the island of Sylt in Northern Germany. This location was chosen because it provided a combination of open sea conditions and shallow water suitable for the injection of poles in the bottom of the North Sea. Reference [36] details the experimental setup and radar-target geometry as well as the antenna array calibration procedure.

Figs.14-15 show the performance of RML, QRML and Fourier beamforming; the latter is used as a reference to judge the tracking performance. Fourier beamforming gives slightly better results than a two-element phase monopulse operating in open loop mode. Fig.14 presents results for a representative set of data files collected for sea state 4 and 5 conditions. The SNR for this representative set of data files was extremely high, about 50 dB. Note that only the last 30 estimates in Fig.14 correspond to sea state 5 conditions. The 130 estimates plotted in Fig.14 correspond to approximately 20 minutes of tracking. Each estimate was obtained from eight snapshots (8.16 seconds) taken at two frequencies: 8.6 and 9.6 GHz. The target range was 9.6 km; the true target height is indicated by the circles on each figure. Note that the snapshots have been integrated over 512 samples (1.02 seconds) to reject clutter.

The tracking performance obtained with the RML (Fig.14a) is excellent. Results in [36] indicate root-mean square tracking errors 5 to 6 times lower than those of Fourier beamforming. This means that the residual specular component still acts as an aid to the RML algorithm while the performance of Fourier beamforming is adversely affected.

Note that the objective function for QRML is formulated in terms of target height. The search for the maximum of the objective function is carried out over only positive values of target height. Therefore very bad estimates that would ordinary lead to negative heights are always indicated as zero target height. For the examples of Fig.14a, the QRML algorithm gave only zero height estimates (not plotted).

The results of Fig.15 are obtained from the only data file collected from a moving target: a German Sea King helicopter. Only approximate target height and range were available for comparison with the estimates. The pilot of the helicopter was asked to start at a low altitude of about 25 m at a distance of (9.5-10 Km), to increase altitude to approximately 300 m while flying towards the ELAT radar and then to gradually decrease altitude back to 25 m at a range of 5 Km. The Sea State was SS3 and the estimated SNR per element was 17 dB. RML gave very good results. In contrast, height estimates obtained by Fourier beamforming have a larger variance; approximately 30% of the estimates are well removed from the true track. QRML gave valid estimates only when the target had sufficient altitude.

The RML algorithm requires a rather high signal-to-noise ratio in order to choose the correct local maximum of the objective function. It is believed that a wider bandwidth,

more frequencies and better calibration would produce a greater difference between ambiguous peaks and thus relax the SNR requirements.

5.2 Tracking in the presence of ducting

This section presents examples of target height estimation enhancement obtained with the method presented above using experimental data in the presence of evaporation ducts. Two representative conditions are considered: duct heights of 9.6 and 5.5 m, respectively, where the degree of confidence on the predicted refraction profile is known to be high. These refraction conditions were selected to show some examples of tracking performance improvement that can be obtained when valid modeling of the prevailing condition is achieved.

Electromagnetic data were collected using a height gain profiler (HGP) developed at the Defense Research Establishment Ottawa (DREO). It consists of a coherent receiver mounted on a vertical trolley which samples the incoming field as it moves up and down along a 18.4-m tower. This equipment can be used to synthesize various array antenna configurations (antenna height and aperture size) by considering portions of recorded signals. Fig.16 shows the HGP measurement setup. A beacon transmitter is used to emulate a target return signal.

HGP measurements were made over Lake Ontario, near Burlington (Ontario), from Nov. 15 to Nov. 21, 1988. The measurement site is shown in Fig.17. The beacon, a continuous-wave X-band transmitter, was mounted on a platform located in the lake at slightly more than 1 km from the Hamilton beach (capital T in Fig.17). The HGP was installed on the Burlington shore. (capital R in Fig.17). The beacon was at 11.5 m above water and the HGP collected the signal over the height interval 7.4 to 25.8 m above water. The range of the propagation path was 11.97 km. Two frequencies (8.6 and 9.6 GHz) and two polarizations were used during the experiment. The bulk meteorological measurements required by WKDMBL were supplied by the Canadian center for inland water (CCIW) which operates a permanent meteorological station on the Burlington Pier which is at about 4 km from the transmitter's platform (capital M, in Fig.17). Wave heights were less than 1 m and so they were neglected in the analysis.

Measurements were processed as shown in the functional block diagram of Fig.18. For each ducting condition, measured meteorological parameters were used as inputs to the

proposed RML system. Signal vectors, **s**, were obtained by extracting signal elements (amplitude and phase) from discrete positions of the recorded HGP signal for several antenna heights specified as input. Arrays so emulated were all made of an evenly spaced 28 elements covering a 1-m aperture. Four array heights were considered for each ducting condition. They were chosen to have a sufficient signal-to-noise ratio (SNR), that is to be distant from interference troughs. In the analysis, we wanted to concentrate on the atmospheric refraction effects exclusively. In practice, a real RML receiver would be capable of coherently integrating incoming signals to provide sufficient SNR in most elevations, which is not possible with the HGP. The influence of the SNR on the RML height estimation is discussed in [1-3].

Table 1 presents the meteorological parameters for the two selected ducting conditions. Fig.19 shows the corresponding refractivity profiles as given by WKDMBL. For Condition 1, antenna heights of 11, 12, 13 and 14 m are considered and for Condition 2 antenna heights of 18, 19, 20 and 21 m are considered. For each antenna height, both horizontal and vertical polarizations were considered.

	Wind speed (m/s)	Air Temp. (C)	Water Temp. (C)	Relative Humidity (%)	Waves Height (m)	Pressure (mbar)	Duct Height (m)
Cond. 1	6.6	5.4	5.4	62.2	0.5	1010	9.6
Cond. 2	3.4	4.1	5.1	67.0	0.5	1025	5.5

Table 1: Meteorological parameters for the two conditions

Resulting target height estimates are plotted in Fig.20. Fig.20(a) shows the results for Condition 1 while Fig.20(b) presents the corresponding results for Condition 2. The true target height is 11.5 m. Circles show estimations obtained using the pair WKDMBL-PCPEM method to compute $\mathbf{f}(h)$ while triangles show estimates obtained under the assumption of normal propagation conditions. The results clearly show the tracking improvement obtained when using an appropriate prediction $\mathbf{f}(h)$ under anomalous conditions. Only three estimates (out of 16) are outside the 1-2 m acceptable error corridor while most of the estimates are far outside that corridor when using previous RML algorithm in which standard propagation condition is assumed. The few unsuccessful estimates may be caused by ambiguities and poor signal-to-noise ratio. Also, it is worth

noting that in each figure the last four data points (at the right) correspond to vertically polarized signals.

6. CONCLUSION and RECOMMENDATIONS

We have presented in this paper a new method for low-angle tracking in the presence of multipath and ducting. The proposed solution is to apply maximum likelihood beamforming to an array radar having frequency agility in combination with a model for representing the multipath and ducting. Obviously the tracking performance will depend on how well the model represents the physical situation. The simulation results indicate that the effects of ducting must be modeled in order to get accurate tracking at ranges greater than roughly 5 km for the typical radar-target geometry encountered in maritime low-angle tracking. However the propagation models are imperfect; there is still some work to be done in the case of rough surfaces. Another difficulty is finding an efficient technique for determining the index of refraction throughout the medium. The difficulties reside in the acquisition of meteorological data and the modeling of the air/sea surface boundary layer.

The results of limited experiments with the HGP are encouraging and indicate that very accurate tracking can be obtained in the presence of multipath and ducting when the propagation conditions are known a priori. However, more extensive experimentation with a real antenna array in conjunction with a meteorological system, where several snapshots can be collected, is required to determine the limitations of the approach in realistic environments. Real-time performance could be obtained by using look-up tables where a large number of scenarios would have been pre-computed.

Computer simulations and experimental results have been used to demonstrate the impact of specular and diffuse multipath on low-angle tracking in standard propagation conditions. These results show that the RML algorithm, in which only specular multipath is modeled, gives the best estimation accuracy. We introduced a new algorithm, QRML, which accounts for both specular and diffuse multipath. Both simulations and experiments indicated a performance advantage for RML in rough sea conditions. This was attributed to the much greater sensitivity to calibration errors of QRML in comparison with RML.

Depending on the environmental conditions we can propose the following solutions:

In standard conditions + specular multipath; use RML with the Kerr model.

In standard conditions + specular + diffuse multipath; use RML with the Kerr model.

In almost diffuse multipath; use phase monopulse with frequency agility.

In ducting conditions; use RML with WKDMBL and PEM.

7. ACKNOWLEDGMENTS

The authors acknowledge assistance provided M.R. Fortin (Laval University), E. Riseborough (DREO) as well as Advanced Information Technology, Applied Silicon Inc., Informission Ltée.

8. REFERENCES

[1] Turner, R.M, Bossé, É., " Maximum Likelihood Tracking Using a Highly Refined Multipath Model ", 21st Asilomar conference on Signals, Systems and Computers, Pacific Grove, CA, Nov.2-4, 1987.

[2] Bossé, É., Turner, R.M, Lecours, M., " Tracking Swerling Fluctuating Targets at Low Altitude Over the Sea ", IEEE Trans. on AES, vol.21, No.5, Sept.1991.

[3] Bossé, É., Turner, R.M., Brookes, D., " Improved Radar Tracking Using a Multipath Model: Maximum Likelihood Compared with Eigenvector Analysis", submitted to IEE Proceeedings, Part F: Radar and Signal Processing.

[4] Schmidt, R.O., " Multiple Emitter Location and Signal Parameter Estimation ", Proc. RADC Spectral Estimation Workshop, pp.243-258, Rome, NY, 1979.

[5] Bossé, É., Turner, R.M., " The Lake Huron Data Base: Characterization and Use for Evaluating Multifrequency Monopulse Tracking Using a Multipath Propagation Model ", DREO Report 1178, June 1993.

[6] Turner, R.M., Riseborough, E., Bossé, É., " Radar Tracking in Multipath: Techniques for Improved Performance ", AGARD Conf. Proceedings 539 on Pointing and Tracking Systems, Seattle, U.S., 12-15 Oct. 1993.

[7] Beard, C.I, " Coherent and Incoherent Scattering of Microwaves from the Ocean", IEEE Trans. on AP, Vol.AP-9, pp.470-483, Sept. 1961.

[8] Beckmann, P., Spizzichino, A., "The Scattering of EM Waves from Rough Surfaces ", Artech House, Norwood, MA, 1987.

[9] Dion, D., " Marine Boundary Layer Model Evaluation by Using a Height Gain Measurement Technique in the Interference Region ", Proceedings of CCECE/CCGEI 1991, Quebec City, Sept. 25-27, 1991.

[10] Jeske, H., "Die Ausbreitung elektromagnetischer Wellen im cm- bis m-Band über dem Meer unter besonderer Berücksichtigung der meteorologischen Bedingungen in der maritimen Grenzschict", Hamburger Geophysikalische Einzelshriften, De Gruyter, Humburg, 1965.

[11] Paulus, R.A., " Environmental Measurements Specification for Radar Propagation Assessment ", NOSC Technical Report, NOSC, San Diego, CA, 92152-5000, 1989.

[12] Low, T.B., Hudak, D.R., " Final Report on the Development and Testing of a Marine Boundary Layer Model ", Kel Research Corporation, Downsview (Ont.), May 1990.

[13] Walmsley, J.L., "On Theoritical Wind Speed and Temperature Profiles Over the Sea With Applications to Data from Sable Island, Nova Scotia", Atmosphere-Ocean, vol. 26, no. 2, pp. 203-233, 1988.

[14] Hitney , H.V., " Hybrid Ray Optics and Parabolic Equation Methods for Radar Propagation Modeling ", Proc. of IEE International Conference Radar 92, Brighton, England, Oct .1992.

[15] Craig, K.H., Levy M.F., " Parabolic Equation Modelling of the Effects of Multipath and Ducting on Radar Systems ", IEE Proceedings-F, Vol.138, No.2, Apr.1991.

[16] Dockery, G.D., " Modeling Electromagnetic Wave Propagation in the Troposphere Using the Parabolic Equation ", IEEE Trans. on Antennas and Propagation, Vol.36, pp.1464-1470, 1988..

[17] Craig, K.H., Levy, M.F., " A PC-Based Microwave Propagation Forecasting Model ", Seventh Intern. Conf. on Antennas and Propagation, ICAP 91, University of York, U.K, 15-18 April, 1991.

[18] Barton, D. K., " Low-Angle Radar Tracking ", Proceedings IEEE, vol.62, no. 6, pp. 687-704, June 1974.

[19] White, W.D., " Low-Angle Radar Tracking in the Presence of Multipath ", IEEE Trans. on Aerospace and Electronics Systems, AES-10, No.6, pp.835-852, Nov. 1974.

[20] Sherman, S.M., " Complex Indicated Angles Applied to Unresolved Radar Targets and Multipath ", IEEE Trans. on Aerospace and Electronics Systems, AES-7, pp.160-170, Jan.1971.

[21] Kesler, J., Haykin, S., " A New Adaptive Antenna for Elevation Angle Estimation in the Presence of Multipath ", Proc. IEEE AP-S Int. Symp., Québec, pp.130-133 June 1980.

[22] Haykin, S., Kesler, J., " Adaptive Canceller for Elevation Angle Estimation in the Presence of Multipath ", IEE Proc. F, Commun., Radar and Signal Processing, vol.130, pp.303-308, June 1983.

[23] Haykin, S., " Array Signal Processing ", Englewood Cliffs, NJ, Prentice Hall , 1985.

[24] Rook, B., Litva, J., " An Improved CHA Algorithm for Tracking Low Angle Targets", CRC Report No. 1356, Communications Research Centre, Ottawa, May 1980.

[25] Bossé, E., Turner, R.M, " Height Ambiguities in Maximum Likelihood Estimation with a Multipath Propagation Model ", 22nd Asilomar Conference on Signals, Systems and Computers, Pacific Grove, CA, Oct. 31-Nov. 2, 1988.

[26] Ballance, W., Jaffer, A.G., " Low-Angle Direction Finding Based on Maximum Likelihood: an Unification ", 21st Asilomar conference on Signals, Systems and Computers, Pacific Grove, CA, Nov.2-4, 1987.

[27] Reilly, J.P., " Nonlinear Array Processing Techniques with Applications to Correlated Multipath ", Ph.D Thesis, McMaster University, Hamilton, Ontario, March 1981.

[28] Haykin, S., Reilly, J.P., " Maximum Likelihood Receiver for Low-Angle Tracking Radar. Part 1: The Symmetric Case ", IEE Proc. F, Commun., Radar & Signal Process., vol.129, pp.261-272, Aug. 1982.

[29] Howard, J.E, " A Low Angle Tracking System for Fire Control Radars ", IEEE Int.Radar Conf. Rec. Arlington, VA, PP.412-417, April 1975.

[30] Ksienski, A.A, McGhee, " A Decision Theoretic Approach to the Angular Resolution and Parameter Estimation Problem for Multiple Targets ", IEEE Trans. on Aerosp. Electro. Syst. vol.AES-4, pp.443-455, May 1968.

[31] Bangs, W.J., "Array Processing with Generalized Beamformers ", Ph.D. dissertation, Yale University, New Haven, CT, 1971.

[32] Kerr, D.E., " Propagation of Short Radio Waves ", Peter Perigrinus, London, 1987. (Originally published by McGraw-Hill in 1951).

[33] Ostrovityanov, R.V., Basalov, F.A., " Statistical Theory of Extended Radar Targets ", Artech House, Dedham, MA, 1985.

[34] Businger, J.A., Wyngaard, J.C., Izumi, Y., Bradley, E.F., "Flux-Profile Relationships in the Atmospheric Surface Layer", J. Atmos. Sci., vol. 28, March 1971.

[35] Imbeau, R., Lecours, M., Bossé, É and Dion, D., "Ray Tracing Calculation Correction for Wave Propagation inside Evaporation Ducts", Proc. of the 1993 IEEE National Radar Conference, Wakefield, USA , April 1993.

[36] Bossé, É., Turner, R.M., Riseborough, E.S ., Brookes , D., " Sylt Project '90 NATO Trials: Analysis of the Canadian Measurements", DREO Report No.1129, Ottawa, Canada, March 1992.

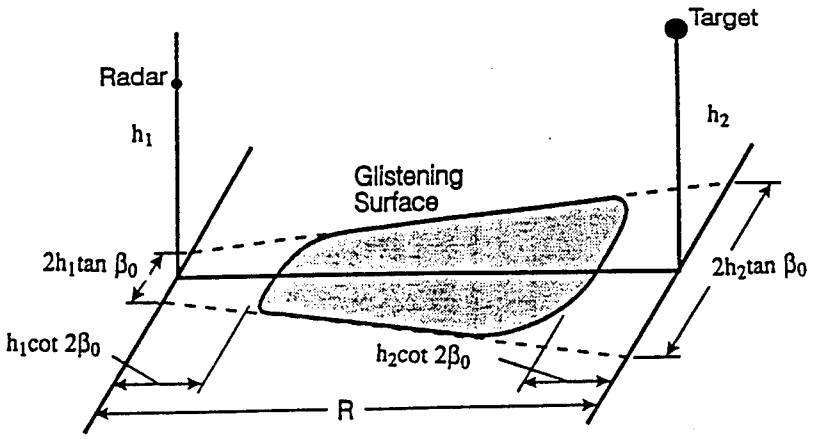

Figure 1: An example of the glistening surface

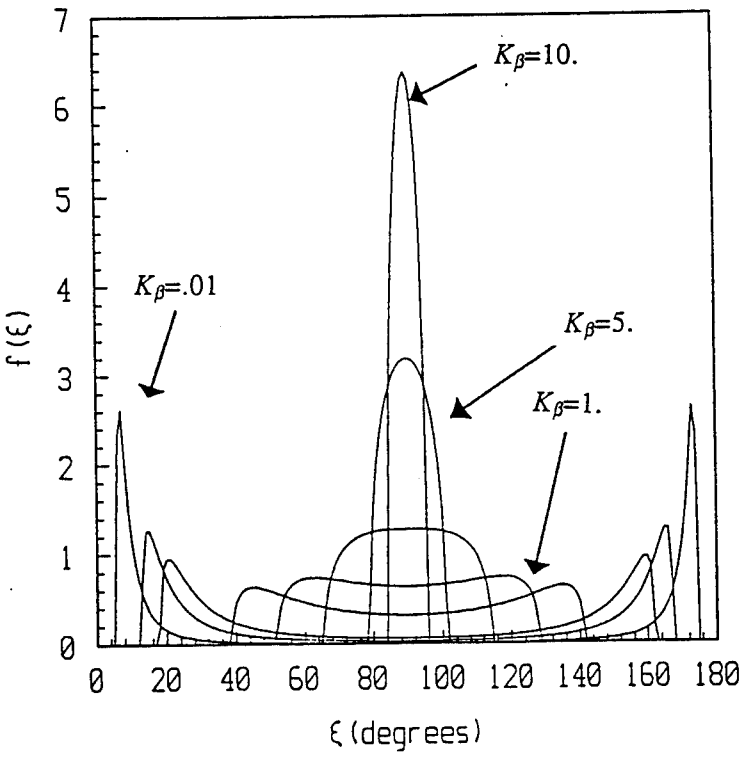

Figure 2: The function $f(\xi)$

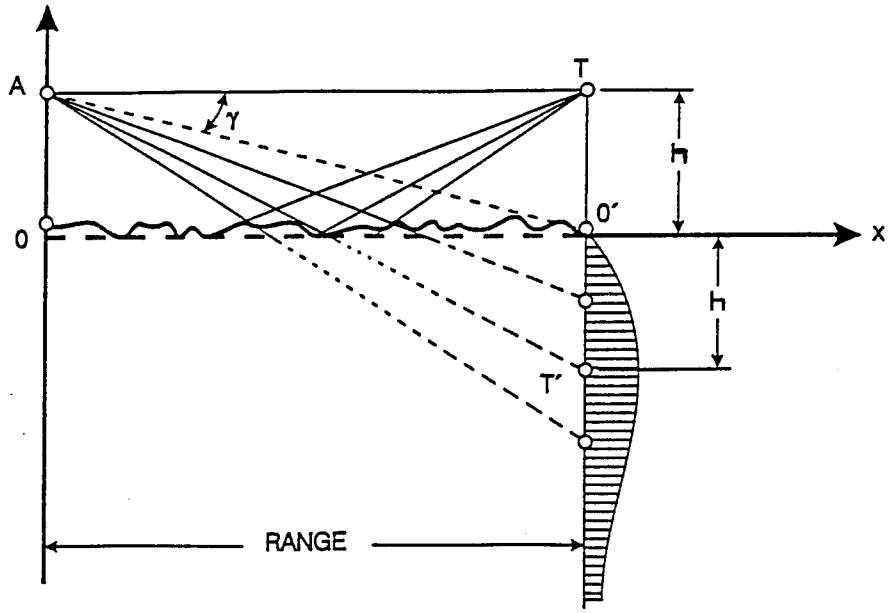

Figure 3: Extension in apparent height of the target due to multiple reflections from a rough surface.

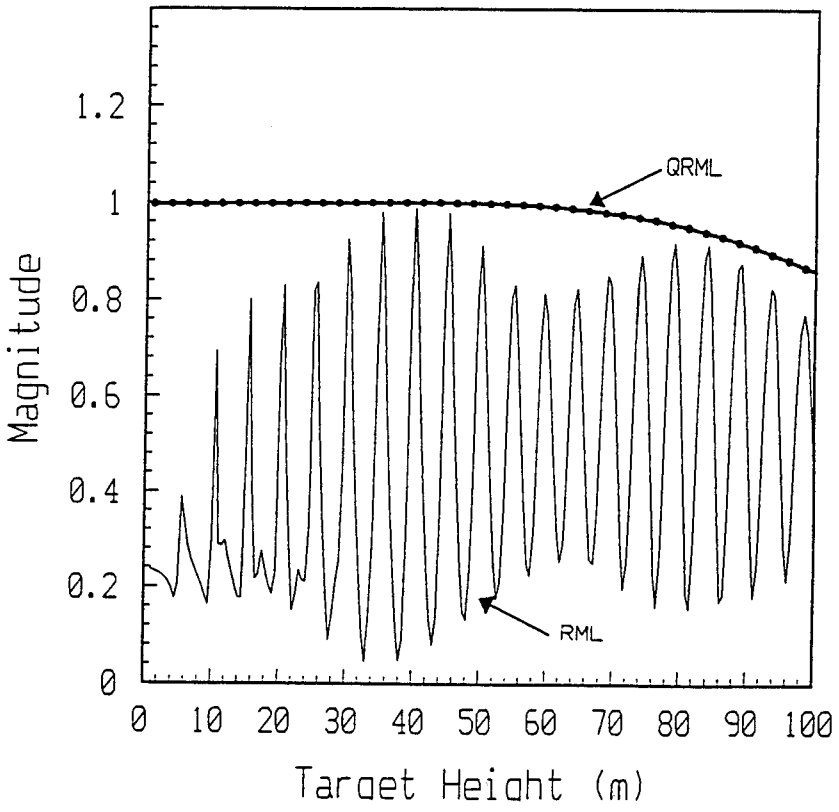

Figure 4: An example of RML and QRML versus height.

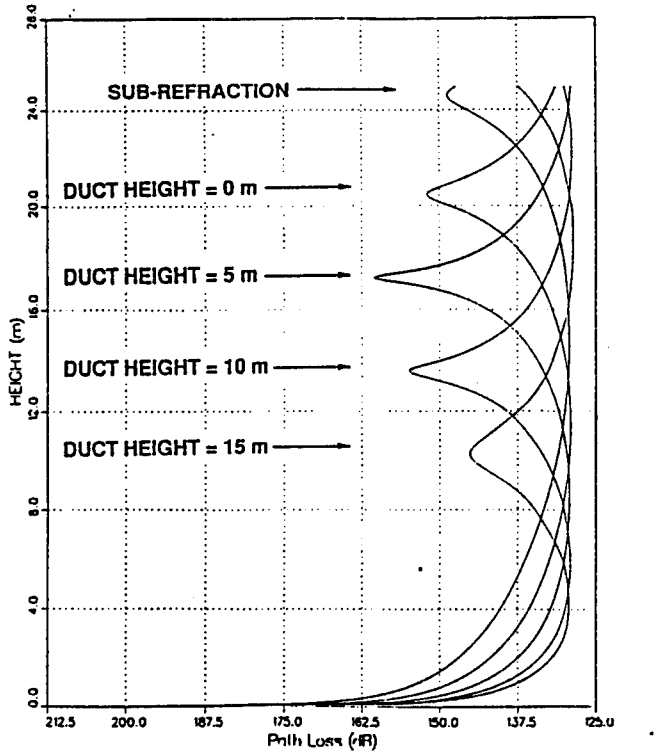

Figure 5: Low-level vertical interference pattern for various duct heights and a subrefractive condition (10 GHz).

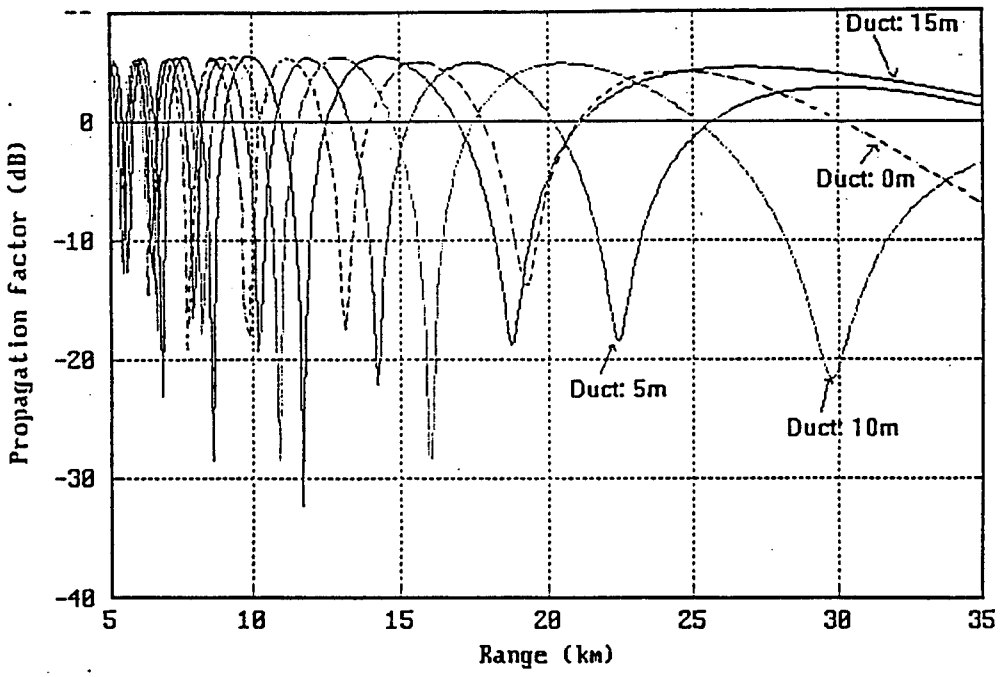

Figure 6: Propagation factor versus range for various duct heights: Freq.=10GHz, antenna height=25 m, pol.=H, BW=1.4 deg., height of the source=20 m.

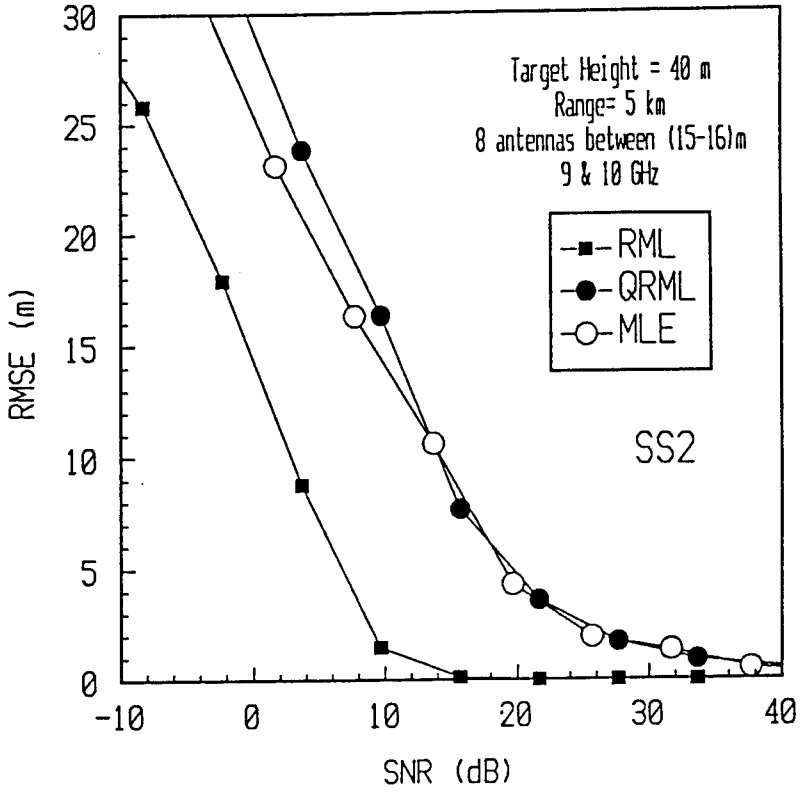

Figure 7: Performance of QRML, RML and MLE when no incoherent multipath is present.

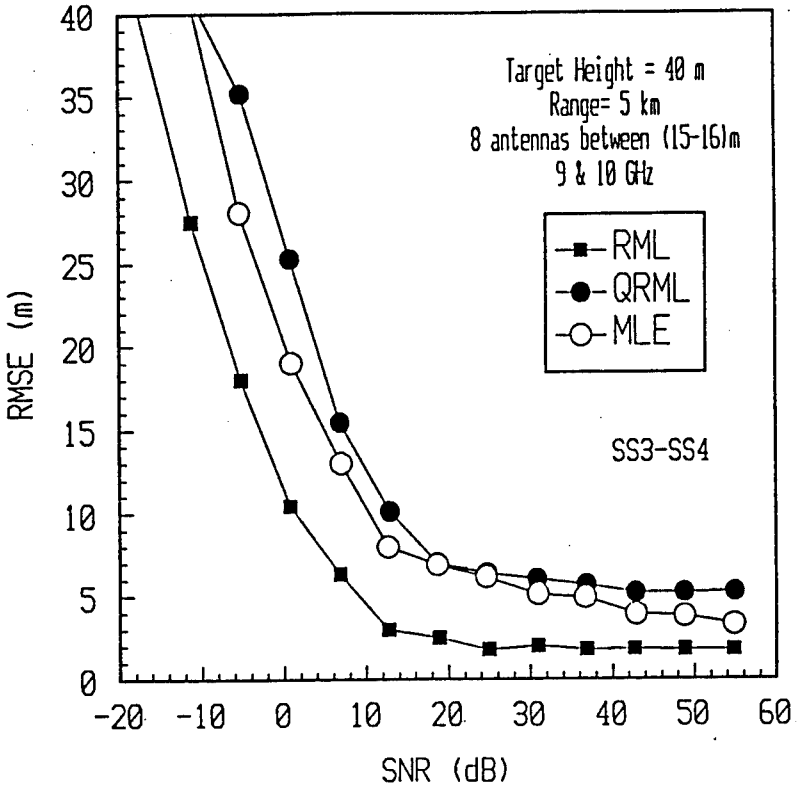

Figure 8: Performance of QRML, RML and MLE when 60% of the incoherent multipath power is from the first Fresnel zone.

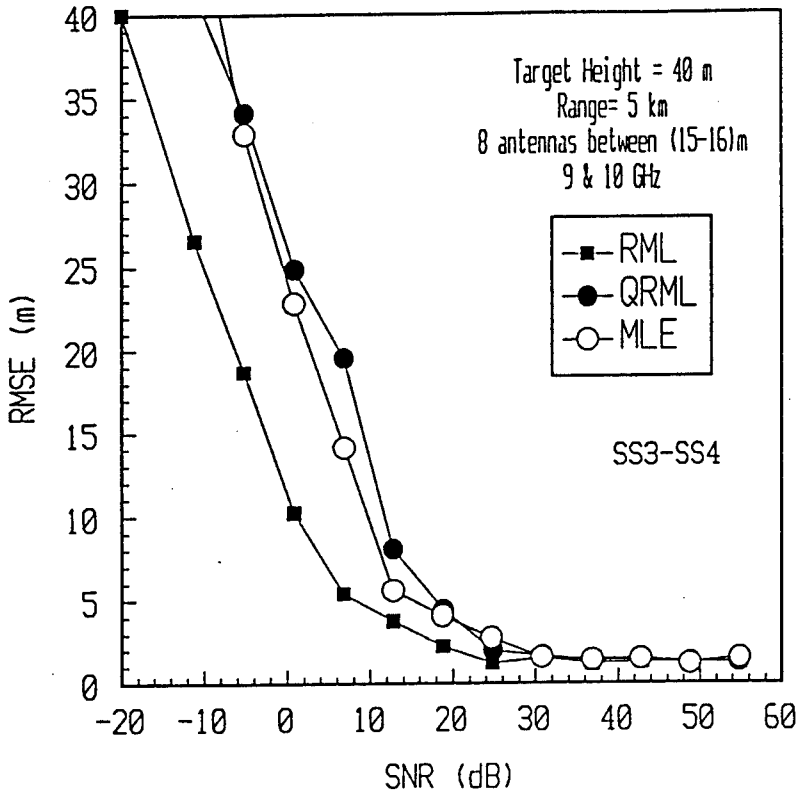

Figure 9: Performance of QRML, RML and MLE when 90% of the incoherent multipath power is from the first Fresnel zone.

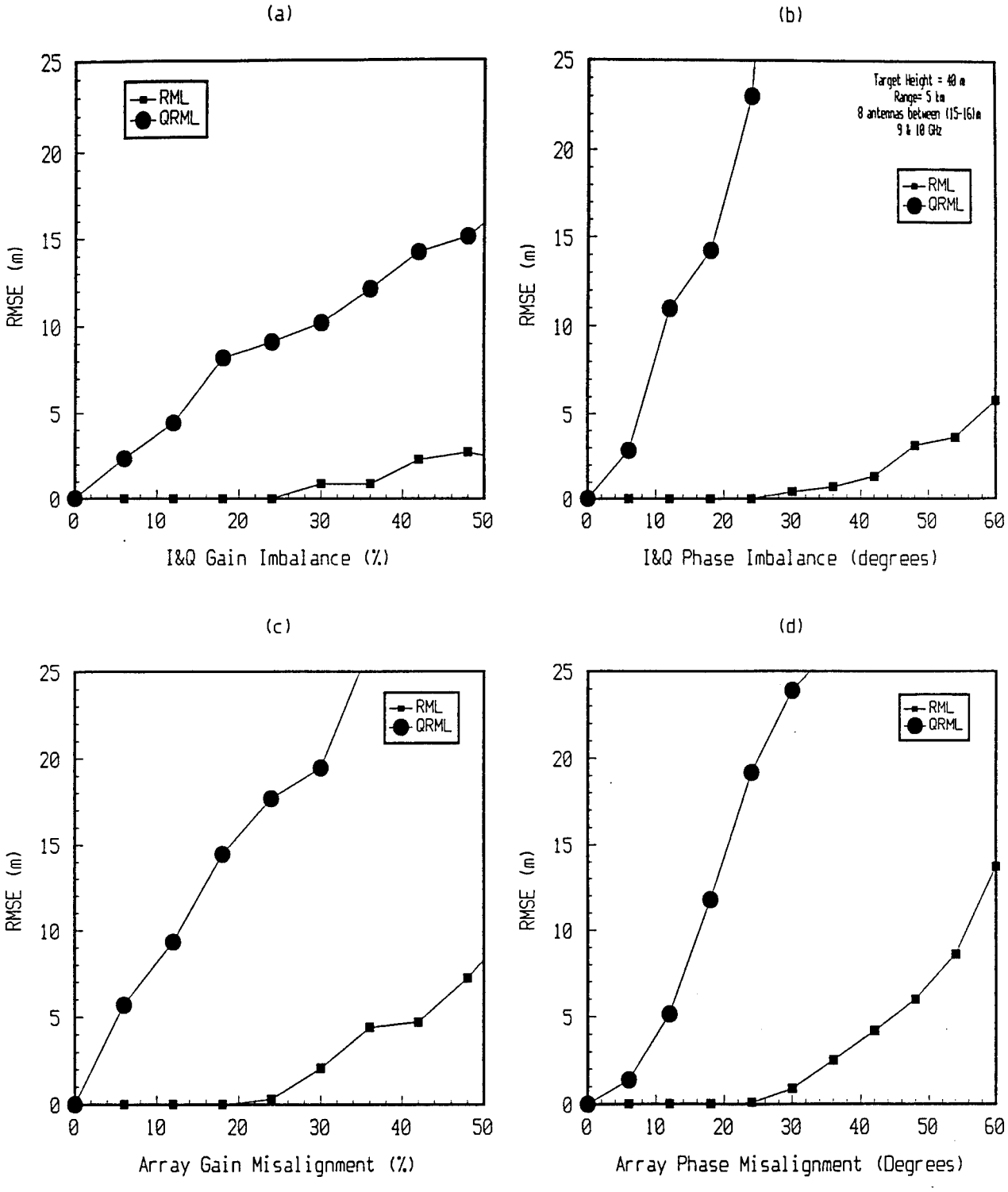

Figure 10: Effects of calibration errors on the performance of QRML, RML and MLE.

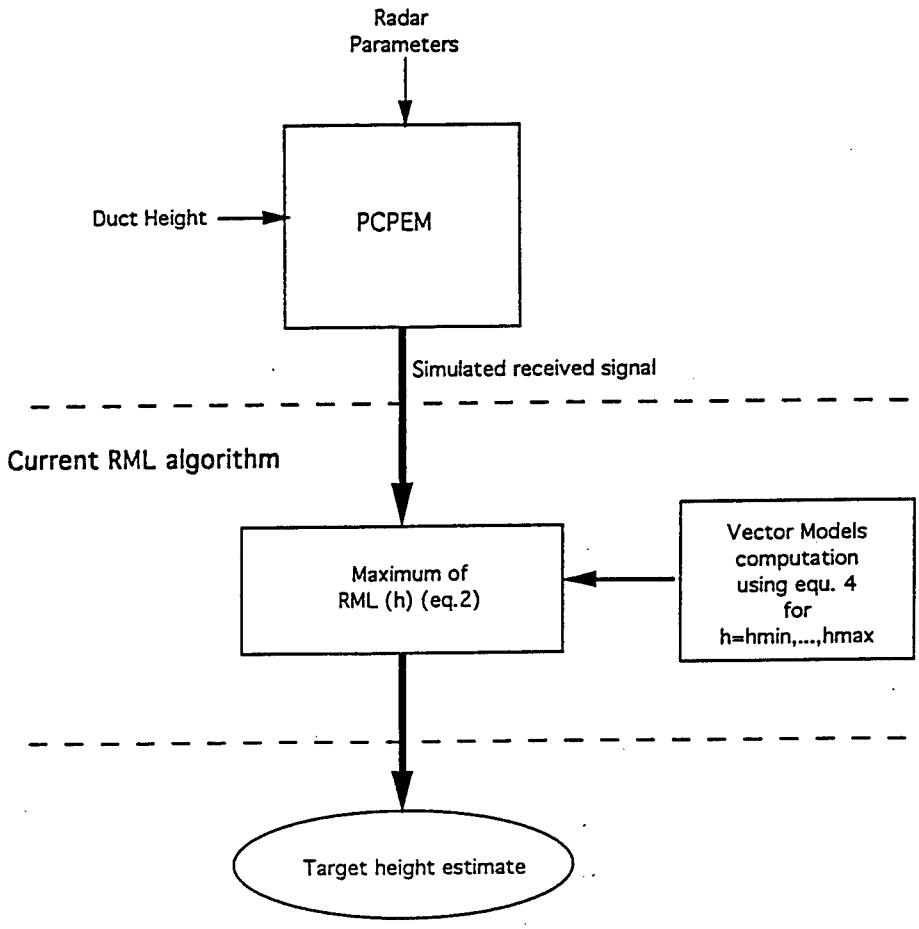

Figure 11: Functional diagram of the simulation.

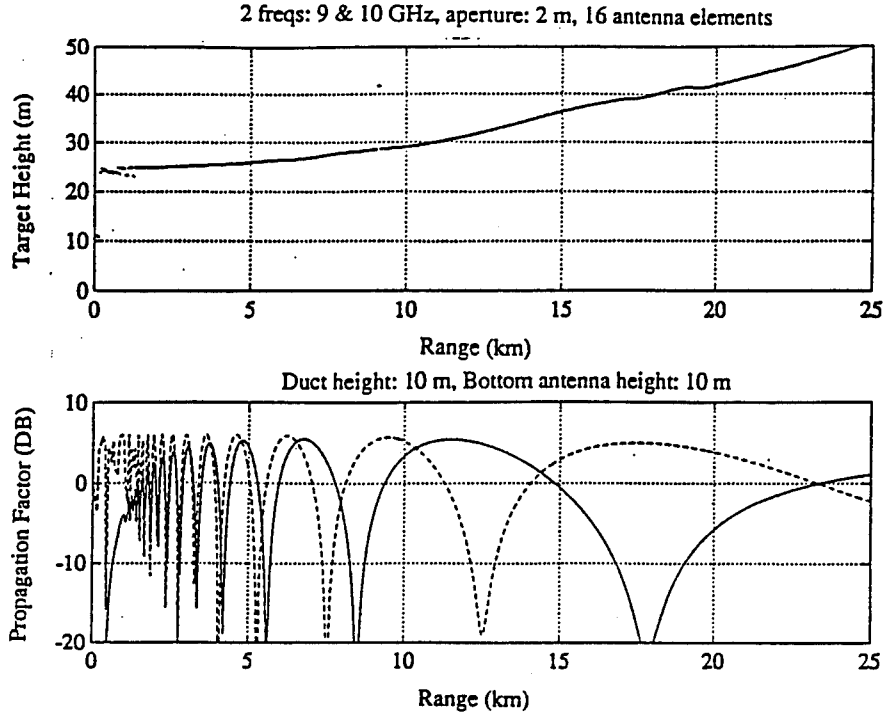

Figure 12: RML target height estimations versus range under a 10-m duct condition and the corresponding propagation factor for a target height of 25 m.

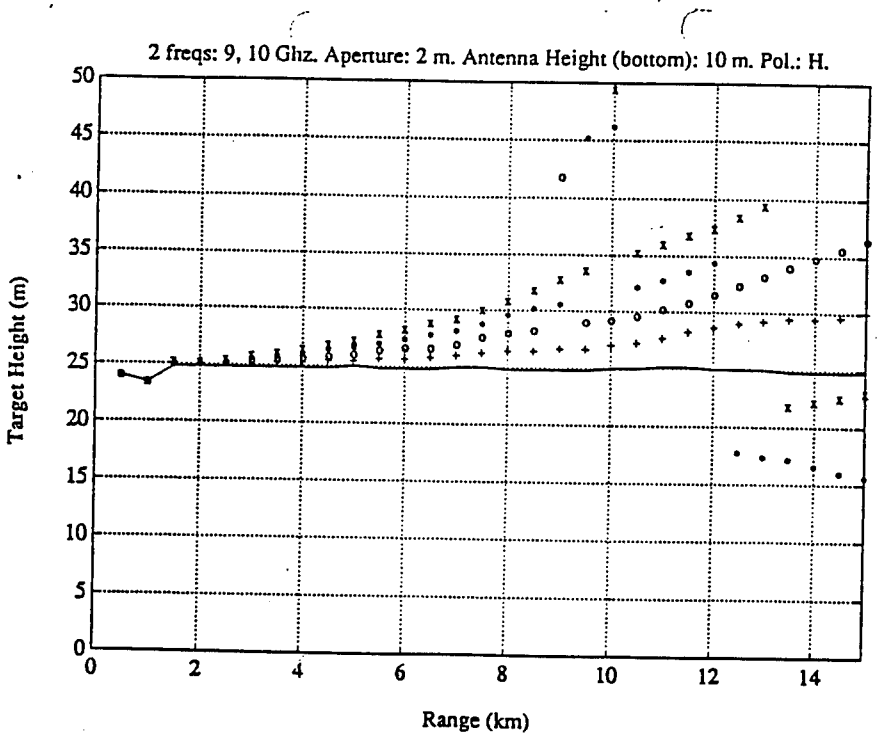

Figure 13: RML target height estimations for duct heights of 0 m (solid line), 5 m (+), 10 m (o), 15 m (*) and 20 m (x) and for a target height of 25 m.

(a)

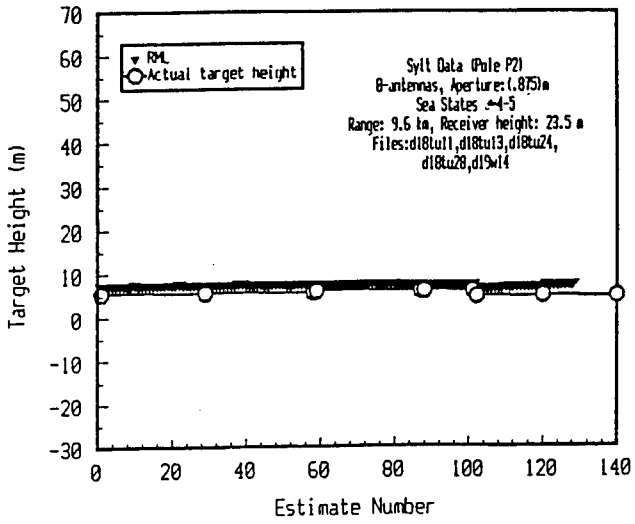

(b)

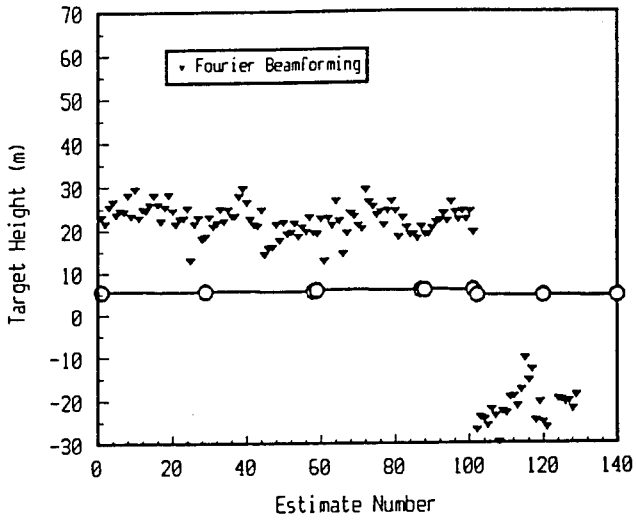

Figure 14: RML and Fourier beamforming tracking over sea states 4 and 5.

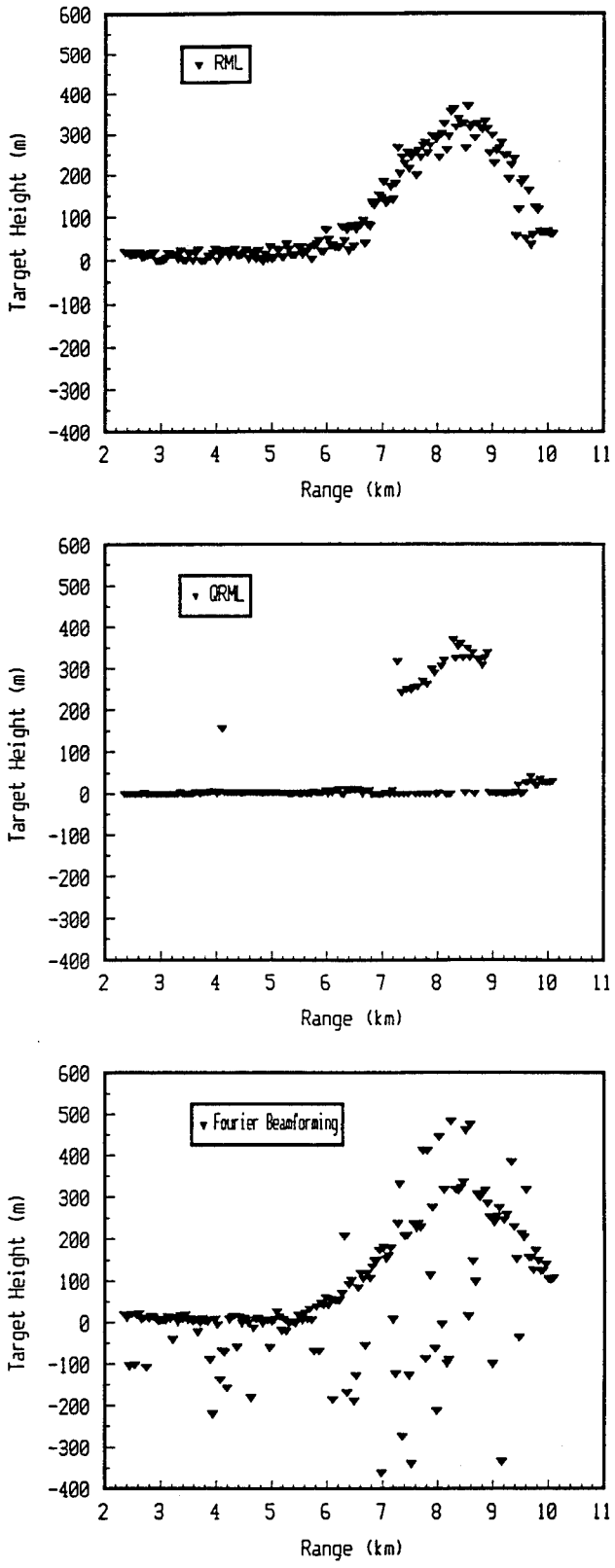

Figure 15: Tracking of a Sea King Helicopter over SS3 sea conditions.

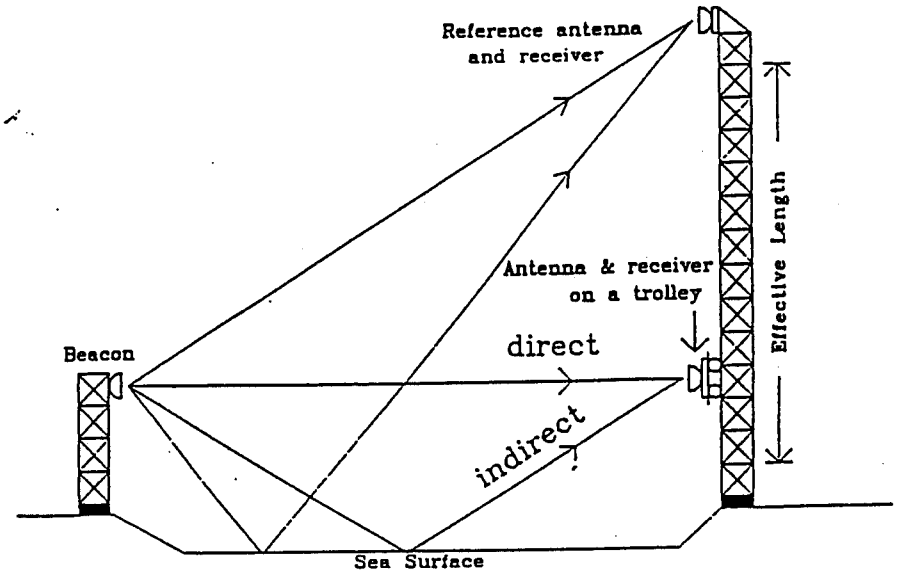

Figure 16: Height gain profiler (HGP) measurements setup.

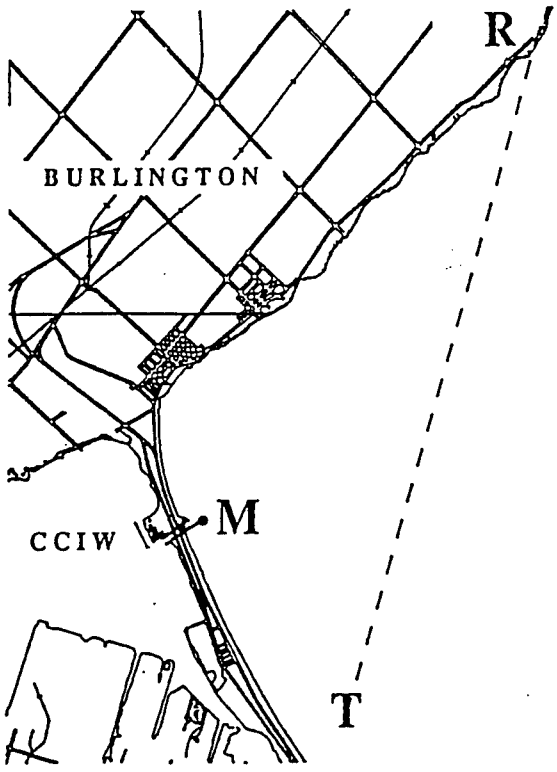

Figure 17: Lake Ontario measurements site.

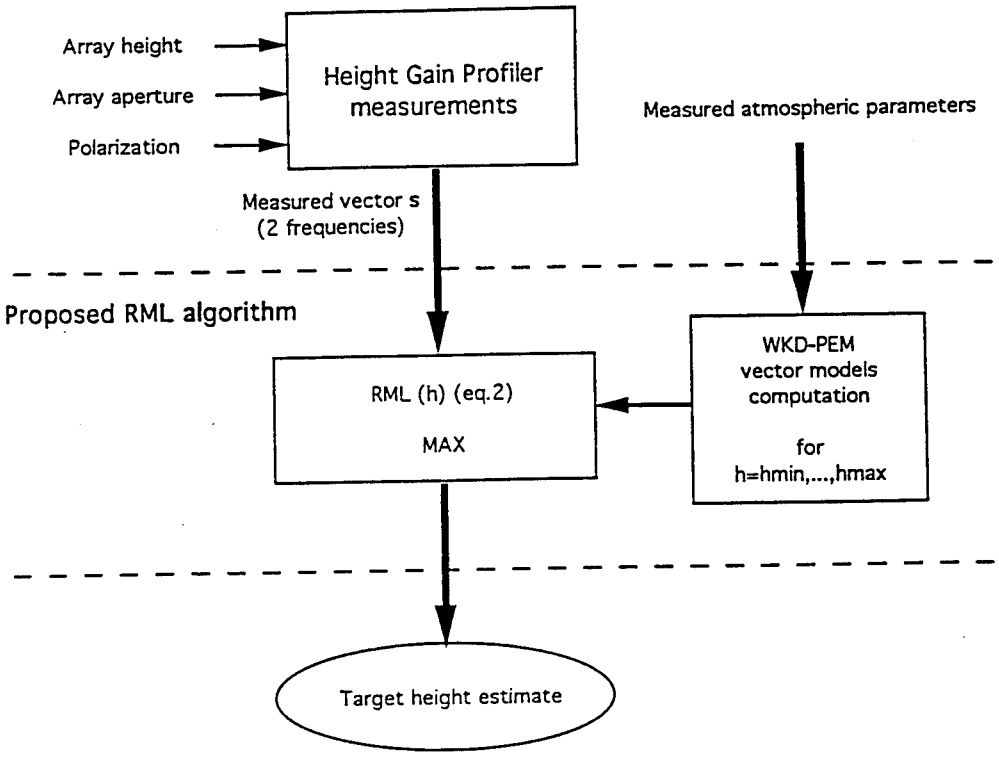

Figure 18: Functional diagram of the analysis of target height estimation using HGP measurements and the proposed RML_WKDMBL-PCPEM tracking method.

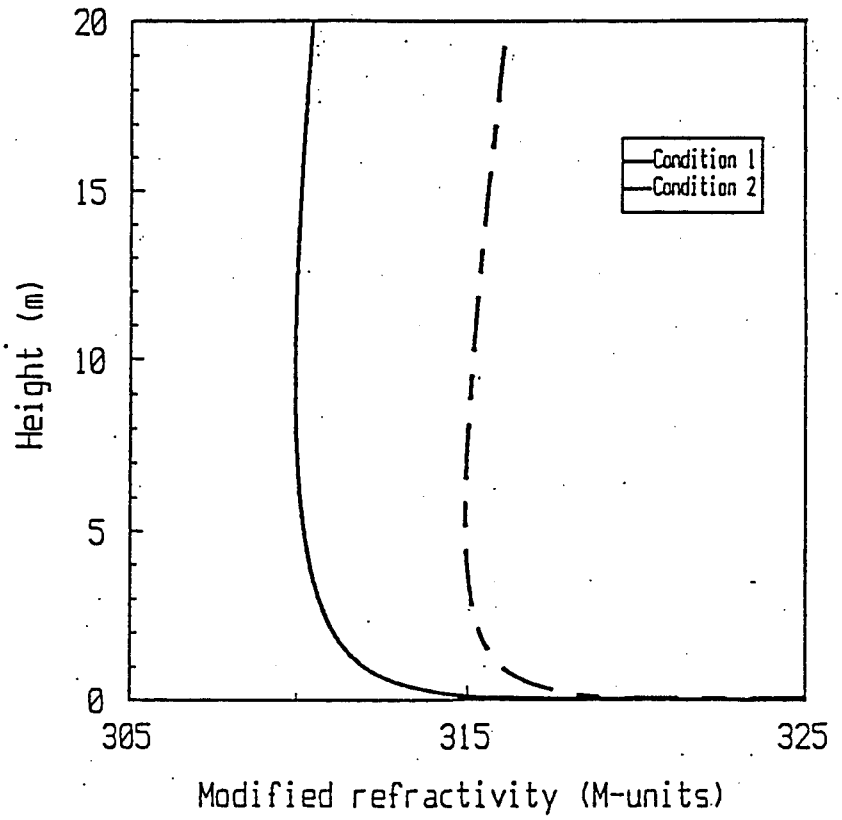

Figure 19: Refractivity profiles corresponding to the ducting conditions considered.

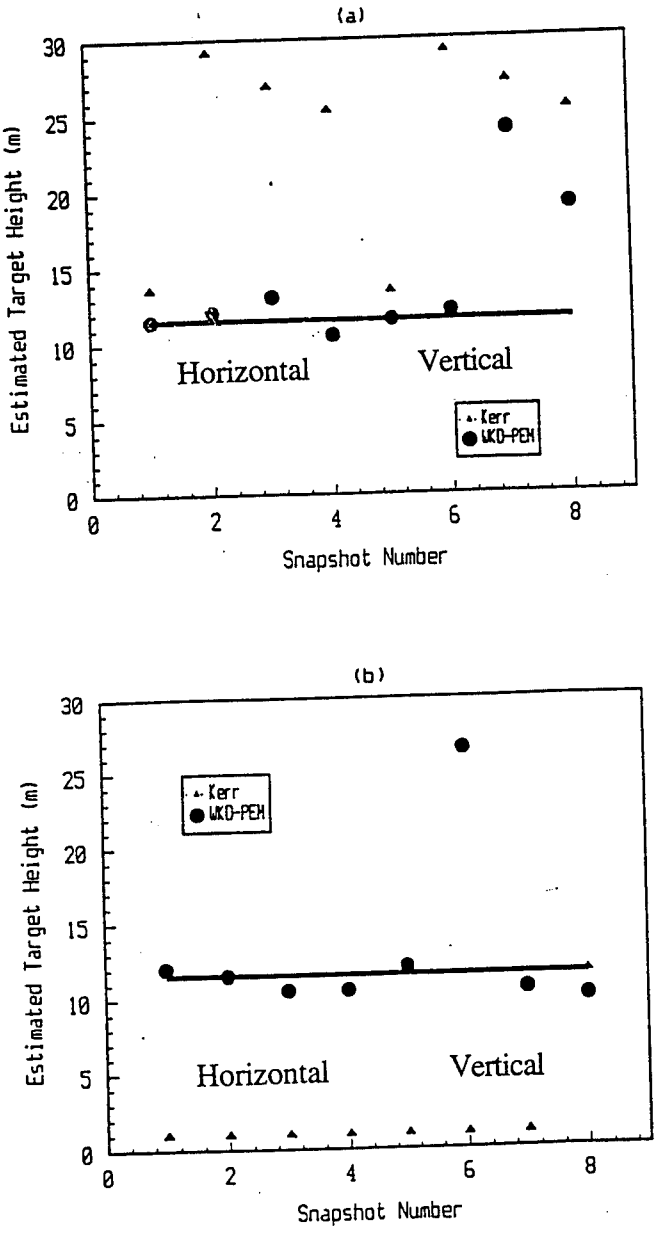

Figure 20: Target height estimations derived from HGP measurements: (a) Condition 1, (b) Condition 2.

DOCUMENT CONTROL DATA

(Security classification of title, body of abstract and indexing annotation must be entered when the overall document is classified)

1. ORIGINATOR (the name and address of the organization preparing the document. Organizations for whom the document was prepared, e.g. Establishment sponsoring a contractor's report, or tasking agency, are entered in section 8.)

Defence Research Establishment Ottawa
3701 Carling Avenue
Ottawa, Ontario, Canada K1A 0Z4

2. SECURITY CLASSIFICATION (overall security classification of the document. including special warning terms if applicable)

UNCLASSIFIED

3. TITLE (the complete document title as indicated on the title page. Its classification should be indicated by the appropriate abbreviation (S,C or U) in parentheses after the title.)

Low-Angle Tracking in the Presence of Ducting, Coherent and Incoherent Multipath (U)

4. AUTHORS (Last name, first name, middle initial)

Eloi Bossé, Denis Dion, Ross M. Turner

5. DATE OF PUBLICATION (month and year of publication of document)	6a. NO. OF PAGES (total containing information. Include Annexes, Appendices, etc.)	6b. NO. OF REFS (total cited in document)
Nov. 94	50	36

7. DESCRIPTIVE NOTES (the category of the document, e.g. technical report, technical note or memorandum. If appropriate, enter the type of report, e.g. interim, progress, summary, annual or final. Give the inclusive dates when a specific reporting period is covered.)

Technical Report

8. SPONSORING ACTIVITY (the name of the department project office or laboratory sponsoring the research and development. Include the address.)

Defence Research Establishment Ottawa
3701 Carling Avenue
Ottawa, Ontario, Canada K1A 0Z4

9a. PROJECT OR GRANT NO. (if appropriate, the applicable research and development project or grant number under which the document was written. Please specify whether project or grant)	9b. CONTRACT NO. (if appropriate, the applicable number under which the document was written)
041LC	

10a. ORIGINATOR'S DOCUMENT NUMBER (the official document number by which the document is identified by the originating activity. This number must be unique to this document.)	10b. OTHER DOCUMENT NOS. (Any other numbers which may be assigned this document either by the originator or by the sponsor)
DREO REPORT 1240	

11. DOCUMENT AVAILABILITY (any limitations on further dissemination of the document, other than those imposed by security classification)

(x) Unlimited distribution
( ) Distribution limited to defence departments and defence contractors; further distribution only as approved
( ) Distribution limited to defence departments and Canadian defence contractors; further distribution only as approved
( ) Distribution limited to government departments and agencies; further distribution only as approved
( ) Distribution limited to defence departments; further distribution only as approved
( ) Other (please specify):

12. DOCUMENT ANNOUNCEMENT (any limitation to the bibliographic announcement of this document. This will normally correspond to the Document Availabilty (11). However, where further distribution (beyond the audience specified in 11) is possible, a wider announcement audience may be selected.)

UNCLASSIFIED

SECURITY CLASSIFICATION OF FORM

13. ABSTRACT (a brief and factual summary of the document. It may also appear elsewhere in the body of the document itself. It is highly desirable that the abstract of classified documents be unclassified. Each paragraph of the abstract shall begin with an indication of the security classification of the information in the paragraph (unless the document itself is unclassified) represented as (S), (C), or (U). It is not necessary to include here abstracts in both offical languages unless the text is bilingual).

This report presents results on recent improvements to the low-angle tracking algorithm based on the Refined Maximum Likelihood (RML) method. Specifically the report describes results obtained for three different models: (1) the RML model; (2) a model which accounts for radar fluctuation of the specular return; (3) a third model which accounts for the effect of ducting. The results indicate that the simple RML model produces better results than obtained by using a model that attempts to account for the incoherent fluctuation in the specular direction. In the case of ducting, under moderate sea state conditions, the parabolic approximation of the Helmholtz wave equation gives accurate tracking while a simple two-way multipath model (Kerr) is used for standard propagation conditions. For very high sea states, phase monopulse with averaging over a number of estimates at different frequencies gives sufficient accuracy for most applications.

14. KEYWORDS, DESCRIPTORS or IDENTIFIERS (technically meaningful terms or short phrases that characterize a document and could be helpful in cataloguing the document. They should be selected so that no security classification is required. Identifiers, such as equipment model designation, trade name, military project code name, geographic location may also be included. If possible keywords should be selected from a published thesaurus. e.g. Thesaurus of Engineering and Scientific Terms (TEST) and that thesaurus-identified. If it is not possible to select indexing terms which are Unclassified, the classification of each should be indicated as with the title.)

Low-angle tracking
ducting
maximum likelihood estimation
radar
multipath

UNCLASSIFIED

SECURITY CLASSIFICATION OF FORM